STRESS-AWARE PERSONALIZED ROAD NAVIGATION SYSTEM

Obai Mandorah

A thesis submitted to the Faculty of Graduate and Postdoctoral Studies in partial fulfillment of the requirements for the degree of

MASTER OF COMPUTER SCIENCE

Ottawa-Carleton Institute for Computer Science
School of Electrical Engineering and Computer Science
University of Ottawa
Ottawa, Canada
September 2019

ABSTRACT

Driving can be a stressful task, especially under congestion conditions. Several studies have shown a positive correlation between stress and aggressive behaviour behind the wheel, leading to accidents. One common way to minimize stress while driving is to avoid highly congested roads. However, not all drivers show the same response towards high traffic situations or other road conditions. For instance, some drivers may prefer congested routes to longer ones to minimize travel time.

Increasingly, drivers are employing Advanced Traveller Information Systems while commuting to both familiar and unfamiliar destinations, not just to obtain information on how to reach a certain endpoint, but to acquire real-time data on the state of the roads and avoid undesired traffic conditions.

In this thesis, we propose an Advanced Traveller Information System that personalizes the driver's route using their road preferences and measures their physiological signals during the trip to assess mental stress. The system then links road attributes, such as number of lanes, speed limit, and traffic severity, with the driver's stress levels. Then, it uses machine learning to predict their stress levels on similar roads. Hence, routes that contribute to high-levels of stress can therefore be avoided in future trips. The average accuracy of the proposed stress level prediction model is 76.11%.

ACKNOWLEDGMENTS

This thesis would not have been possible without Allah (SWT). First and foremost, I would like to thank Him for giving me health, strength, and patience through the whole journey.

Special thanks to my supervisor Prof. Hussein Al Osman for his incredible guidance and support through this whole experience. It was a true privilege to earn knowledge under his supervision.

Also, I'm very grateful to my family especially to my parents for their incredible care and support. They have always been by my side encouraging me to achieve my dreams.

Many thanks to my friends who helped me and inspired me during my study.

Finally, special thanks go to my sponsor: Umm Al-Qura University.

TABLE OF CONTENTS

Abstract ii

Acknowledgements iii

List of Figures vi

List of Acronyms vii

Chapter 1. Introduction *1*

1.1 Background **1**

1.2 Motivation **2**

1.3 Problem Statement **2**

1.4 Contributions **3**

1.5 Thesis Outline **3**

Chapter 2. Literature Review and Related work *4*

2.1 Literature Review **4**

2.1.1 What is Stress? 4

2.1.2 Using HRV to assess stress 6

2.2 Related Work **8**

2.2.1 Studies on Driver Stress and Driving Behavior 8

2.2.2 Studies on Routing with Driver Preferences and Behaviour 10

2.2.3 Physiological Measurements for Driver Stress 13

2.3 Gap Analysis **14**

Chapter 3. Proposed System *16*

3.1 System Requirements **16**

3.2 Methodology **16**

3.3 System Architecture **17**

3.2.1 Here Maps API 20

3.2.2 Recommender Component 21

3.3 Stress Detection Setup **24**

3.3.1 Window size and overlapping 28

3.3.2 Stress Index (SI) Smoothing 29

3.5 Database Tables **30**

Chapter 4. Results, Evaluation and Discussion *33*

4.1 Data Collection **33**

4.1.A Subjects selection criteria 33

4.1.B Context classification 34
4.1.C Algorithms used for ML 35

4.2 Results 39
4.2.1 Evaluation metrics for stress level prediction 42
4.2.2 Stage (A): Results on Individual Dataset 43
4.2.3 Stage (B): Results on Group Dataset 55

Chapter 5. conclusion and future work ***59***

5.1 Conclusion 59

5.2 Limitations and Future Work 59

References ***61***

Appendix ***66***

LIST OF FIGURES

Figure 1: Example of R-R Intervals 6
Figure 2: Proposed System Architecture 19
Figure 3: Sequence Diagram for Obtaining a Route Recommendation Based on a Source and Destination 20
Figure 4: The questioner from which the app will configure the route for the user 23
Figure 5: Screenshots from the navigation app 24
Figure 6: Zephyr Bioharness sensor [left], Misfit Vapor smartwatch [right] 25
Figure 7: Comparison between ECG and PPG signals 25
Figure 8: Comparison between RAW/filtered PPG and ECG signals while driving 26
Figure 9: Empatica E4 wristband [side and back] 27
Figure 10: Polar H10 ECG sensor 28
Figure 11: Shifting HRV windows over road segments for smoothing the SI 29
Figure 12: The Entity Relationship Diagram of the system 30
Figure 13: Stress Comparison between Driver_1 and Driver_6 (Home-to-Work same route) 40
Figure 14: A Comparison between the AVG trip Stress Index based on the trip orientation 41
Figure 15: Example of Raw Trip Data 66
Figure 16: Example of Trip Stress Table 66
Figure 17: Example of stress prediction on Weka 67

LIST OF ACRONYMS

ATIS: ADVANCED TRAVELER INFORMATION SYSTEM

HR: HEART RATE

HRV: HEART RATE VARIABILITY

IBI: INTER BEATS INTERVALS

BPM: BEATS PER MINUTE

ECG: ELECTROCARDIOGRAPHY

GSR: GALVANIC SKIN RESPONSE

PPG: PHOTO-PLETHYSMOGRAPHY

LF: LOW FREQUENCY

HF: HIGH FREQUENCY

ML: MACHINE LEARNING

ANS: AUTONOMIC NERVOUS SYSTEM

SNS: SYMPATHETIC NERVOUS SYSTEM

PNS: PARASYMPATHETIC NERVOUS SYSTEM

ST: SKIN TEMPERATURE

SCR: SKIN CONDUCTANCE RESPONSE

SI : STRESS INDEX

SL : STRESS LEVEL

CHAPTER 1. INTRODUCTION

1.1 Background

Driving can be a stressful task. The experienced mental stress can lead to aggressive driving behaviour, which eventually can cause accidents. Many studies have found connections between highly congested roads and the aggressive driving stimulated by stressors [1]–[4].

Increasingly, drivers are employing Advanced Traveller Information Systems (ATIS) while commuting to both familiar and unfamiliar destinations, not just to obtain information on how to reach a certain endpoint, but to acquire real-time data on the state of the roads and avoid undesired traffic conditions.

In this thesis, we propose a personalized routing system that aims to minimize the amount of mental stress experienced by drivers. Personalized routing is not a novel idea in itself as much research has already been done in that regard [5]–[8]. To the best of our knowledge, none of the existing work proposes an approach in which personalized routing takes into account the driver's stress.

Each individual has their own preferences in terms of road attribute (i.e. wide roads, countryside, highway, etc.), thus the mental stress in response to the driving stimulus can differ substantially from one individual to another. Hence, a system that monitors the stress response during driving and associates it with road characteristics can better provide a personalized routing experience that aims at reducing frustration on the road.

Evidently, the driver's overall stress may be caused by a number of other factors, namely work, home, other personal matters, or other drivers on the road[1][9], all of which are out of our control and are therefore out of the scope of this thesis. Our focus is to minimize the stress related to road and traffic conditions, based on the user's preferences.

There are numerous studies that discuss driver stress and its effects on driver behaviour [1], [4], [9]–[22]. Elevated stress levels can lead drivers to engage in aggressive maneuvers, which can lead to horrific accidents. However, a very low stress level can mean a lack of attention or drowsiness, which can also cause traffic accidents. Therefore, an engaged driver experiences a small amount of mental stress that is associated with attention.

1.2 Motivation

Many commercially available ATIS can accurately estimate the trip travel time and traffic conditions. Yet, they do not account for the driver's mental state. Despite the customizability options they provide (e.g. avoid tolls, avoid highways, minimize travel time, and minimize distance travelled), they do not cater to the individualized driver's preferences that can aid in stress reduction. We propose an approach to monitor the driver's physiological signals to measure their stress levels while driving. We will collect road characteristics, such as traffic conditions, road width, speed limit, etc., and consider the subject's road preferences (preferred road attributes), such as highways versus city roads, long routes with less stop-and-go versus shorter routes with many intersections, and wide roads versus narrow ones. This information will enable us to determine the driver's stress levels over each road segment, and eventually for the whole trip, and help us gain insight into how the individual responds to their surrounding environment. Subsequently, the driver's preferences will be taken into account and will influence the routing process.

1.3 Problem Statement

Through the years, ATIS, such as Google Maps and Apple Maps, have progressed remarkably in terms of accurately calculating the optimum route for the user and providing an accurate estimate of the travel time. However, studies on how the user reacts to various types of roads and road conditions are essential in establishing the optimal route for an individual. An ideal system should learn from the

driver's behavioural and physiological responses and adapt the recommended route accordingly. However, current ATIS do not consider the user's biofeedback at any time and the recommended routes are therefore the same for all, despite individual preferences.

1.4 Contributions

We summarize our contributions as follows:

- We designed and implemented an ATIS using the HERE Maps API. The system allows the user to specify their road preferences and learns about their stress response to different encountered road conditions. Consequently, the ATIS can attempt to minimize mental stress by taking into account previously learned information about the driver's stress response.
- We collected a dataset on uncontrolled road conditions and used machine learning methods to analyze the user's stress on each road segment, to predict stress levels on similar roads for each individual.

1.5 Thesis Outline

The remainder of this thesis is organized as follows:

Chapter 2 presents the literature review of related studies on stress detection and routing based on driver preferences. It concludes by suggesting a combination of the two fields.

Chapter 3 illustrates in detail the design of the proposed system and the system architecture. It also shows the methodology used for data collection and stress index calculation.

Chapter 4 explains the system's implementation as well as technical details for both the hardware and software components. In addition, it presents the Machine Learning (ML) on stress prediction.

Chapter 5 provides the conclusion and summarizes our vision of future works

CHAPTER 2. LITERATURE REVIEW AND RELATED WORK

2.1 Literature Review

2.1.1 What Is Stress?

The definition of stress can vary depending on the context, either in medicine, social sciences, anthropology, psychology, or engineering. Nevertheless, any discussion about stress is incomplete without reference to the outstanding work of Hans Selye, considered by many as the father of stress research. He states that "*Stress is the nonspecific response of the body to any demand.*"[23], whether that demand produces pain or pleasure. Moreover, Gillian H. ***et*** al.[24] consider stress as "*a process by which a stimulus elicits an emotional, behavioural and/or physiological response, which is conditioned by an individual's personal, biological and cultural context*". Our bodies react to stress through our Autonomic Nervous System (ANS), which branches into two sub-systems; the Sympathetic Nervous System (SNS), and the Parasympathetic Nervous System (PNS). The SNS is responsible for our body's "fight or flight" reactions, in response to external or internal stressors. It triggers blood glucose production (to charge the muscles) and pupil dilation (to focus on targets), and increases heart rate (to satisfy the body's need for extra oxygen to fuel the run or fight response). Hence, the SNS stimulates the organs that are controlled by the ANS. Conversely, the PNS controls the body's "rest and digest" actions, which are linked to recovery. The PNS constricts pupils, stimulates digestion, and decreases heart rate. Both SNS and PNS control the same organs but with inverse impacts. The SNS is needed to conquer the short-term stress circumstances, such as running from a predator or fighting an intruder, while the PNS is needed for long-term survival, such as growing healthier and stronger. Thus, a balance between the two systems is essential to maintain a healthy nervous system. To gain insight into the ANS activity, we can collect philological measures on the organs that it controls. Hence, by monitoring how it controls these organs, we can infer information about its status. The typical physiological signals that

are reflective of ANS activity are Blood Pressure (BP), Skin Conductance Response (SCR) (also known as the Galvanic Skin Response (GSR)), Skin Temperature (ST), and Heart Rate Variability (HRV). In particular, HRV was proven to be an accurate non-intrusive measure for stress [25]. Alharthi [26] developed a context-aware stress prediction system that can analyze the user's HRV signals to measure and visualize stress. Moreover, it uses machine learning to predict stress and provide tips to mitigate stress. Al Osman, Eid, and El Saddik [27] developed a system that monitors the user's mental and physiological status for elevated stress using HRV measures.

Many studies have proposed a variety of routing and road suggestions approaches. For instance, Yuan et.al.[28] proposed a system that leverage taxi driver's experience through their GPS logs into building a system that calculates faster routes than regular ATIS. Liebig et.al. [29] introduced a system that uses a stream of sensors in a smart city to estimates the traffic in the future and calculates the best route to avoid highly congested roads that could appear. Moreover, researchers have proposed road navigation systems that consider the driver's behaviour and road preferences to recommend routes. For example, Letchner, Krumm, and Horvitz [8] developed a system called TRIP that takes into account the driver's individual driving preferences and the driver's past GPS logs in order to plan future routes. Another approach presented by Adler and Blue [6] is to apply Artificial Intelligence (AI) techniques to learn from repetitive commuters about their road choices, and therefore provide more intelligent routing assistance.

The navigations systems described above do not support features for stress monitoring and prediction aimed at reducing the driver's frustration. Nonetheless, the effects of stress on driver behaviour well is documented in the literature. Wiesenthal and Hennessey [16] studied the effect of mental stress on driver behaviour. They found that congested roads showed higher rates of aggressive driving and a greater number of accidents. In such situations, the study concluded that repeated exposure to stressful situations was linked with heightened aggression and road rage.

2.1.2 Using HRV to assess stress

In order to obtain Heart Rate Variability (HRV) from ECG signals, R peaks detection is required to measure the R-R intervals, also known as Inter Beats Intervals (IBI). The R peak refers to the most prominent impulse in the ECG record during a heart cycle. It coincides with the depolarization of the ventricles. The difference between the Heart Rate (HR) and HRV is that HR reflects the average heart Beats Per Minute (BPM) (which corresponds to the number of R peaks within a minute long ECG record) while HRV provides a deeper insight into the time variability between successive heartbeats (Figure 1). For example, an HR of 60 BPM does not necessarily correspond to a heartbeat every second. For instance, there may be more heartbeats in the first 30 seconds compared to the last.

A. R-R Intervals

From the successive raw R-R intervals within an ECG records, we can derive an HRV signal where we can perform time and frequency domain analysis [30] to infer some information about the status of the ANS.

Figure 1: Example of R-R Intervals

B. HRV parameters

We list below the most commonly calculated time-domain HRV parameters:

- SDNN (ms): Standard deviation of the R-R intervals

- RMSSD (ms): Square root of the mean squared differences between successive RR intervals
- NNxx: Number of successive RR interval pairs that differ more than xx ms
- pNN50 (ms): Percentage of pairs of adjacent RR intervals differing by more than 50 ms.
- STD HR (beats/min): Standard deviation of instantaneous heart rate values
- TINN (ms): Baseline width of the RR interval histogram

Moreover, we list the frequency-domain HRV parameters:

- Peak frequency (Hz): VLF, LF, and HF band peak frequencies
- LF (Hz): Low frequency (by default 0.04-0.15 Hz)
- HF (Hz): High frequency (by default 0.15-0.4 Hz)
- VLF (Hz): Very low frequency (by default 0-0.04 Hz)
- LF/HF (ms^2): Ratio between LF and HF band powers

C. Stress Deviation Factors

According to various studies, HRV in response to stress differs between individuals due to age, genetic composition, environment and gender[31][32][25]. J. Taelman et.al. [25] examined the role of mental stress influence on heart rate and heart rate variability in a group of 28 subjects. The researchers found that over 85% of the subjects showed an increase of the LF/HF measure in under increased mental stress (which is linked to sympathetic activity), compared to when they were at rest. Ryan et.al. [32] ran a study on (n=83) subjects to examine the effect of gender and age on HRV. The study concluded that women demonstrate more complexity in HRV than men. Liao et.al [31] in a study conducted with 1,984 healthy subjects aged between 45 and 64 years, found that the HRV spectral indexes (LF, HF, and LF/HF) are related to sex, age, and race.

2.2 Related Work

2.2.1 Studies on Driver Stress and Driving Behaviour

Researchers have investigated the influence of road conditions and traffic congestions on driver stress levels. Westerman and Haigney [17] conducted a study with a large sample of participants (2806 drivers) to examine driver stress and assess driving behaviour. The paper concluded that men tend to be more aggressive drivers than women, but with fewer lapses. Conversely, driver stress levels were not influenced by gender. Age does have an impact on driving behaviour, with fewer violations by older drivers, despite the fact that the 'dislike of driving' increased and 'alertness' decreased with age. Additionally, the researchers noted a strong relationship between driver stress levels and aggression. Finally, the authors established a correlation between high driver stress and driving violations.

Wiesenthal and Hennessy[16] described driving as a source of everyday stress, similar to time pressure, job concerns, and financial considerations. The growing number of vehicles on the roads has triggered a competition for space, increased congestion levels, and created many potential sources of frustration, irritation, and stress. Moreover, the researchers argued that psychological and physiological health is adversely affected by traffic congestion, i.e. increased heart rate, arousal, and high blood pressure. Furthermore, highly congested roads show higher levels of aggressive driving and a greater number of accidents. The authors noted that repeated exposure to stressful situations has been linked with intensified aggression and road rage. The researchers divided the behaviour responses of the subjects into six categories, namely, aggressive, information seeking, planning, minor self-destructive, distraction, and relaxation techniques. According to the study observations, in the high-congestion conditions, only aggressive behaviours were predictive of driver stress levels. Those who were more aggressive were more likely to exhibit elevated stress levels.

In their study, Hill and Boyle[18] focused on understanding how different driving tasks and roadway conditions may influence the stress perceived by drivers. The data were collected from a survey that analyzed drivers' stress in various road, traffic, and weather-related scenarios. The results unveiled four scenarios that were classified in terms of 1) weather, 2) visibility, 3) interactions with other drivers, and 4) driving tasks. The study separated stress into two dimensions: State Stress (influenced by an external situation or event), and Trait Stress (from factors that reside within an individual). Behavioural patterns, such as aggressiveness, Type A personalities, and other personality traits, were also considered to have an impact on stress levels. The authors found a strong relationship between personality and stress, which is often related to differences observed in gender and age. Also, there were other factors that induced stress levels, such as time constraints and unfamiliarity with driving conditions.

Gulian et al.[1] collected and analyzed the daily behaviours and feelings of drivers while driving in the form of a checklist. This study examined day-to-day cognitive and affective reactions to routine journeys and to specific traffic events by drivers who completed the Driving Behaviour Inventory (DBI) questionnaire. It examined the following hypotheses:

(1) Driving stress levels are constant over a one-week period provided that no major traffic incident(s) and/or life event(s) occur.

(2) There are differences between the reported morning and evening driving stress levels, mainly due to fatigue.

(3) Driving stress is determined by the interactions between a user's reactions towards traffic and other road users, and factors extrinsic to driving.

The study subjects were divided into two groups. The first group was asked to complete the DBI diary for seven days, in the morning, in the evening, and after their last car ride. The second group, however, was asked to complete the diary for five days only, but in a fixed sequence of Monday to Friday. Using

a general factor as a stress scale, the Daily Driving Stress scale (DDS) was then constructed with items loading 0.40 or above, where levels were calculated every morning and evening, of each day**.** The study showed that there is a strong relationship between age and experience and driving stress. Compared to older drivers with more experience, younger and less experienced drivers reported higher stress levels. The diaries completed twice-daily showed that the levels of driving stress reported in the evenings were almost always higher than those reported in the mornings. Interestingly, the most stressful day was just before the weekend (day 4). They found that driving stress resulted from the continuous interaction of intrinsic and extrinsic factors to driving, mediated by individuals' general and specific attitudes towards driving.

2.2.2 Studies on Routing with Driver Preferences and Behaviours

Amar, Drawil, and Basir [33] proposed a system that recommends a route influenced by a driver's preferences and road information obtained from an ATIS. The trip planning process is executed in two stages: 1) Feasible road segments are identified and assessed based on the travellers' routing preferences. 2) An optimization process through which the traveller's hard demands (constraints) are the principal factors used to determine the optimum route. There are two types of inputs for the decision module in the Behavior Driven Trip Planner system: 1) Traveler's trip constraints (i.e. trip time, trip budget). 2) The cost of each road segment. Based on personal preferences, the recommendation module assesses each road differently for each user. For example, if there are two different users, both of them departing from the same location and going to the same destination, but each having different road preferences, i.e. one of them prefers driving on highways while the other does not, one prefers a road without traffic lights or stop signs while the other does not mind them. The recommender system will then provide the two drivers with different paths, based on their individual road preferences. An additional goal of the system is to minimize the amount of congestion on the roads, while also alleviating driver frustration as much as possible.

Hadjali, Mokhtari, and Pivert[34] used a fuzzy set theory framework to modulate the user's road preferences and plan a route for the user. fuzzy sets are used as a modelling framework for the purposes of flexibility and uncertainty, and here it is used for route planning queries (RPQ). The author categorized the user's preferences into three groups: 1) Spatial preferences, which focus on the user's wish to take or avoid a particular type of road, such as "avoid secondary roads". 2) Global preferences, that focus on the general properties of a road, like comfort, length, duration or safety, such as "prefer a fast route". 3) Spatio-temporal preferences, which consider a combination of a place and time, such as "avoid the city center around noon". Similarly, Mokhtari et al. [35] also proposed a route planner that deals with complex user preferences by using a fuzzy set approach to balance the positives and negatives of the user's demands.

In an early attempt to include driver preferences into trip planning with an ATIS, Letchner, Krumm, and Horvitz [8] introduced the Trip Router with Individualized Preferences (TRIP), which uses GPS data logged by drivers to estimate the traffic, road speeds, and driver preferences. It determines that when a driver takes a route multiple times, even if it is not considered the optimal route at the time of the query, it is flagged as the favourite route for that individual. The study compared four different metrics: 1) Driver's usual route. 2) Shortest distance route. 3) Fastest route according to the GPS estimation. 4) MapPoint route.

Yuan et al. [28] used taxi drivers' GPS logs to leverage their expertise at maneuvering around dynamic traffic. A Variance-Entropy-Based Clustering method was then proposed to estimate the trip time between two points in various timelines. Finally, based on that graph, they computed the fastest customized route for the user. During a three-month period, they collected real-time data from over 33,000 taxis, and then assessed the system with artificial experiments and in-field evaluations. They claim that their system (T-Drive), when compared to the competitors, was able to produce 20% faster routes (on average), for 50% of the attempts.

Martinez et al. [5] incorporated an Extreme Learning Machine to personalize the driver assistance system and learn from the driver's behaviour. The authors proposed "an individualized and non-intrusive monitoring system for real-time driver support".

Dia [36] presented an agent-based method to analyze individual driver behaviour after they were given real-time traffic information. The study observed and analyzed the response of the drivers under congested roads via behavioural surveys. They used a Belief-Desire-Intention framework to model the driver behaviours under varying contexts. The author used two types of preferences: 1) Revealed preferences (RP) data, which is the actual behavioural response to expected or unexpected reported delays**;** 2) Stated preferences (SP) data, which reports the driver's behaviour during a simulated ATIS scenario.

Ziebart et .al [37] introduced PROCAB, which is a method for Probabilistically Reasoning from Observed Context-Aware Behavior using the maximum entropy principle within the inverse reinforcement learning framework. They incorporated the route preferences of over 20 taxi drivers with more than 100,000 collected miles to train the model and evaluate their system performance. They also conducted a survey of 21 college student drivers to examine the variety of route preferences and contextual factors that affect route choices. The survey provided contextual situations to choose from, namely: early weekday morning, morning rush hour, noon on Saturday, evening rush hour, immediately after snowfall, and night-time. Furthermore, the preferences for each of the different driving situations were weighted on the following five-point Likert scale: (1) very strong dislike, avoid at all costs; (2) dislike, sometimes avoid; (3) don't care, doesn't affect route choice; (4) like, sometimes prefer; (5) very strong like, always prefer. Mainly, the system is used to learn the driver's behaviour to predict the turn and the route to a given destination with an accuracy of up to 93.2% and 82.6% respectively.

Papinski, Scott, and Doherty [38] focused on a group of drivers during home-to-work commute and compared the planned routes with the ones chosen without GPS planning. The authors used GPS data

to record the planned routes, where for the ATIS they used a diary to confirm the trips' start and end times. There were 31 participants in this study, and one-fifth of them tended to deviate from the planned route. Most of the individuals disclosed that they preferred to minimize the travel time and the number of stoplights/signs, as well as avoid traffic congestions. They also showed a liking for straightforward roads.

Park et al.[7] proposed an adaptive route guidance system that learns from the driver's preferences and behaviours. The authors used the C4.5 algorithm to generate a decision tree for the learning process then ran simulation experiments with real-time information to evaluate the system's prediction accuracy.

2.2.3 Physiological Measurements for Driver Stress

There is a bulk of research that examines a subject's stress while driving. The stress detection method is usually based on the analysis of physiological signals like electrocardiogram (ECG), electrodermal activity (EDA), and respiration. Rigas, Goletsis, and Fotiadis [39], Ji, Zhu, and Lan [40], and Vhaduri et al.[41] showcased how to monitor the driver's stress using physiological sensors. Keshan, Parimi, and Bichindaritz [42] demonstrated how to use machine learning to detect a driver's stress with an accuracy of 88.24% when detecting the three classes of stress: low, medium and high, using the ECG signal. Begum[43] summarized other studies on sensors used for stress detection in several aspects (i.e. main goal, sensor type, methods used to detect stress, parameters and sensor measurements).

Although there are many studies that used PPG signals to accurately calculate HRV, some of them used wired equipment [44], which makes it intrusive, while others used it in a controlled environment [45], which limits the study compared to real-life scenarios. Also, some attached the sensor

to the steering wheel [46], which makes it prone to movements, while other studies used two different PPG sensor nodes on the body [47], which makes it less convenient for the driver.

2.3 Gap Analysis

Table 1 presents a comparison between the related works in this chapter that focuses on the following aspects:

1) Main objective of the system (i.e. monitoring the driver route, predicting the user driving behaviour, adapting to driver's behaviour in route selection)
2) Stress Detection Measurements (if there is any).
3) Type of experiment conducted to assess the system (i.e. Controlled roads, Stress Surveys from drivers, GPS logs from Taxi drivers or study volunteers, Simulations experiments on real-time network)

Table 1: Related Work Comparison

Related Work	Main Goal	Stress Detection Measurements	Type of Experiment
Gulian et al.[1]	Monitoring stress	Self reports	Commuting to work
Park et al.[7]	Monitoring route selection, predicting and adapting to route selection behaviour	None	GPS logs, Simulation
Letchner, Krumm, and Horvitz [8]	Monitoring the behaviour	None	GPS logs
Wiesenthal and Hennessey [16]	Monitoring stress and behaviour	Self reports	Controlled (Pre-selected) roads
Westerman and Haigney [17]	Examining the psychometric properties correlation between DBI and DBQ	Self reports	Stress Surveys
Hill and Boyle[18]	Examining the Correlation between driving conditions and stress level	Self reports	Stress Surveys
Yuan et al. [28]	Monitoring and adapting to driving behaviours	None	Taxi drivers GPS logs, Simulation

Ziebart et .al [37]	Monitoring and predicting driving behaviour	None	Taxi drivers GPS logs
Amar , Drawil, and Basir [33]	Monitoring and adapting to behaviour	None	Simulation
Mokhtari et al. [35]	Monitoring and adapting	None	Simulation
Dia [36]	Monitoring the behaviour	None	Surveys, Simulation
Papinski, Scott, and Doherty [38]	Monitoring route selection	None	GPS logs, Surveys
Rigas, Goletsis, and Fotiadis [39]	Monitoring stress	ECG, GSR, and respiration	GPS logs, CAN-bus
Ji, Zhu, and Lan [40]	Monitoring and predicting stress	Facial and eye-tracking	Simulation
Vhaduri et al.[41]	Monitoring and predicting stress	ECG, GSR, and Self reports	GPS logs
Keshan, Parimi, and Bichindaritz [42]	Monitoring and predicting stress	ECG, EMG, GSR, and respiration	Controlled (Pre-selected) roads
The proposed system	Monitoring, predicting, and adapting to driving behaviour and stress	HRV and self reports	Commuting to and from work

Previous studies presented route calculation based on road conditions and the driver's preferences. However, they did not consider the driver's physiological signals during the trip (to analyze stress for example) to personalize route calculation for individuals. Also, to the best of our knowledge, no study presented route calculation with stress level prediction as a cost factor.

CHAPTER 3. PROPOSED SYSTEM

In this chapter, we discuss the proposed system, presenting a general overview of the stress monitoring and provide design and implementation details.

3.1 System Requirements

In this section, we highlight the features that our system supports based on the gap analysis in section 2.3:

- Calculating the route based on the driver's preferences.
- Monitoring the driver's stress during the trip.
- Connecting user's stress level with road's attributes.
- Predicting the individual's stress level on similar roads.

3.2 Methodology

To personalize the routing for each individual, the user first needs to answer a few questions to determine what he/she likes/dislikes in terms of road attributes. These questions allow the system to better understand the user and therefore personalize routing. When the user requests a route to a destination, the calculation for the best route takes the user's preferences into consideration, as well as real-time traffic information, to assess each possible route against the user's preferences. Moreover, the system constantly collects physiological information to analyze stress levels during driving. The stress levels are stored in a user's database. After a sufficient number of trips, the system uses the stored stress information to train a machine-learning algorithm to predict the user's stress on new roads with similar road attributes to those in the driver's history. Hence, the system not only personalizes to the user's

preferences, but also takes into account historical stress information to attempt to minimize the stress level of the driver.

3.3 System Architecture

(Figure 2) describes the architecture of the proposed system. The system is composed of three high-level modules:

- Backend: This module stores user preference and stress information and recommends routes.
- Frontend User Interface (UI): The user interacts with the UI to use the system. The user creates an account, enters preferences, and receives a turn-by-turn navigation information through this module.
- ECG Sensor: This module collects ECG information through a sensor connected to the user's body, pre-processes the signal, and forwards it to the Backend via a Bluetooth connection.

The Backend is composed of several components:

- Controller: This component receives all incoming inputs from the UI and ECG Sensor and forwards it to other backend components for further processing.
- Preference: This component receives user preferences information entered through the UI and forwarded through the controller. It stores this information in the Preferences Database. Therefore, this component simply provides a layer of separation between the Controller and the Preferences Database (as it is the convention in software architectures).
- Stress Estimator: This component receives the ECG information from the ECG sensor and forwarded it through the controller. It processes the physiological information to estimate the stress level of the user. In particular, it collects the R-R intervals from the ECG record, which is then used to calculate the Heart Rate Variability (HRV) needed to analyze the driver's stress.

It also receives the road attributes from the Here Maps API. The road attributes are 1) Road Name, 2) Number of Lanes, 3) Speed Limit, 4) Time of driving on each road segment, 5) Traffic Severity. The road attributes and stress level associated with them (stress level obtained when the driver was going through a road that has these attributes) are stored in the Stress Database.

- Recommender: This component recommends the route to the user based on the information it retrieves from the Here Maps API, Preferences Database, and Stress Predictor. The Here Maps API provides the list of possible routes between a source and a destination. The Preferences Database provides a report on the user's preferences and the number of times the user has travelled through each road in the route, and the Stress Predictor provides the stress level for each route. Hence, the Recommender component takes into account the preferences and predicted stress levels on a route to issue its recommendation. It achieves the stress prediction through its machine learning model. (Figure 3) presents a sequence diagram of the recommender system's operation in response to a request for a route originating from the Front End UI and propagating through the Controller to the Recommender component.

- Stress Predictor: This component uses a machine-learning model to predict the stress level on a route given the historical data stored in the Stress Database. It receives a list of candidate routes from the Recommender component and outputs an average stress level for each route.

- Here Maps API: This is a REST API that allows the proposed system to communicate with the HERE Maps cloud to obtain navigation information, including a list of possible routes, and step-by-step directions.

- Preferences Database: This database stores the user's road preferences. This information is obtained from the user directly through a questionnaire. Moreover, this Database stores the

number of times a road has been travelled by the user. The system keeps track of this information to assess whether a user is familiar with a road along the route.

- Stress Database: This database stores the road attributes and stress levels associated with them.

Given that the system must be personalized per subject, we must collect routing data annotated with the stress information for each subject. This way, we can make predictions about the driver's stress level for various routes during routing.

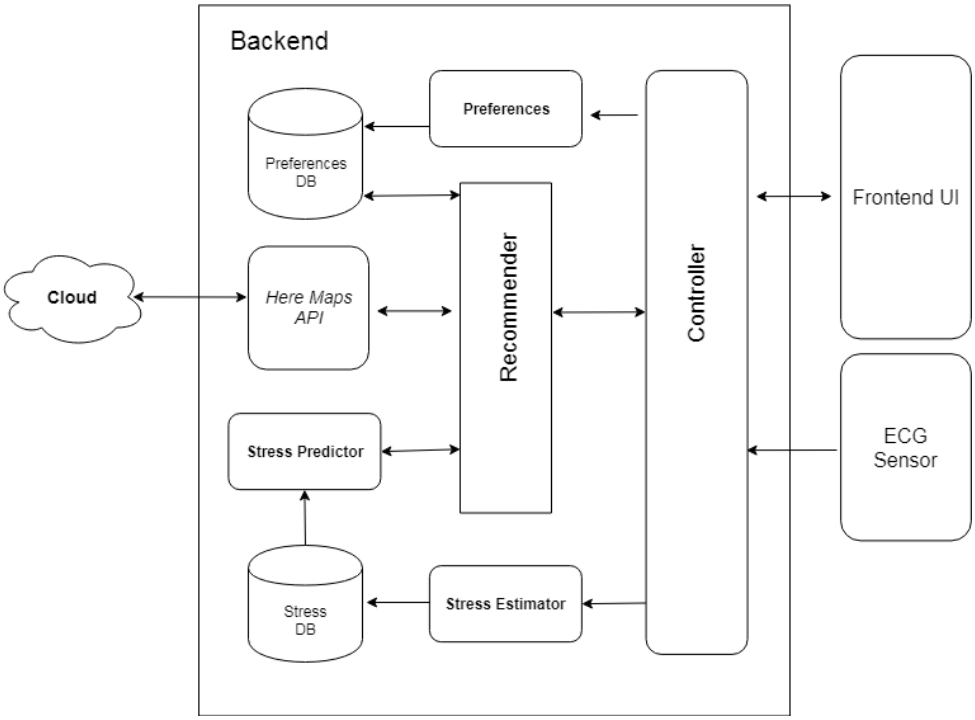

Figure 2: Proposed System Architecture

To collect the driver's preferences and populate the Preferences Database, during account creation, the system presents a questionnaire that use a Likert scale ranging from 1 to 5, where 1 indicates a strong dislike/avoid at all costs and 5 indicates a strong like/always prefer; these questions were influenced by previous works that assessed driver stress[16],[24],[37]. The questions are shown in (Figure 4).

Although our system focuses on minimizing the total cost of the trip for the user, it handles the provided information in different ways, given that the recommender system predicts the user's stress.

Thus, it efficiently distributes the travellers on different roads, according to road attributes (i.e. number of lanes, number of intersections) and time of travel (i.e. rush hour) as well as user preferences (i.e. if the user do not mind taking a longer route but with less traffic).

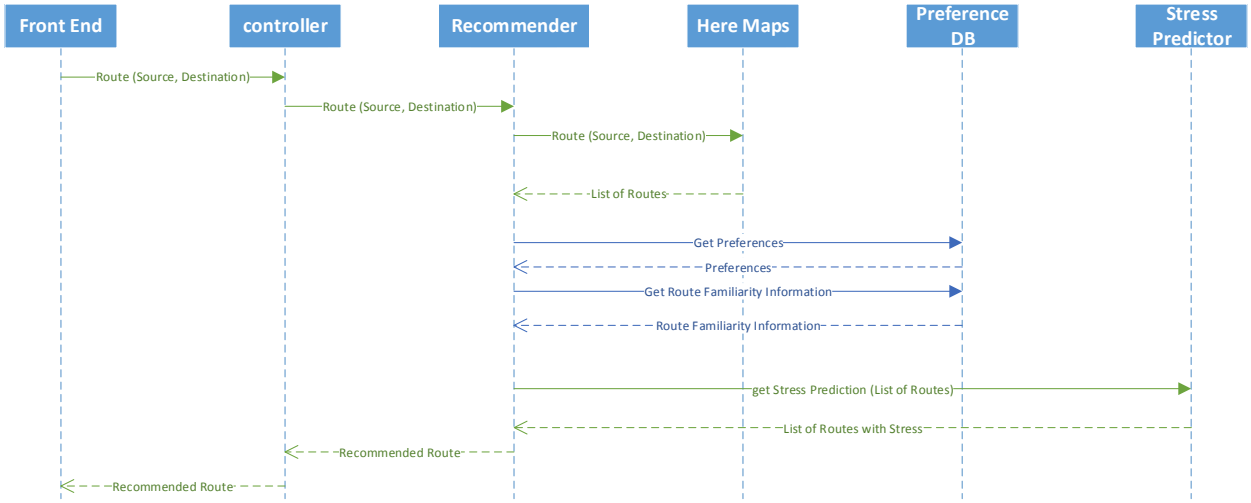

Figure 3: Sequence Diagram for Obtaining a Route Recommendation Based on a Source and Destination

3.2.1 HERE Map API

Google Map is a well-known app for navigation, business reviews, and many other features. Therefore, it may appear obvious to develop a navigation app with an added layer of user preferences and physiological feedback using Google Map API. However, Google Map API has many limitations, for instance, it does not provide real-time navigation and voice guidance with its API. If a developer wants to use Google map, they must design their own voice guidance and arrows and plot the waypoints on the maps, and develop many other needed features for navigation; this makes it a time-consuming process. HERE map API offers all of the missing features for free, for a limited number of transactions per month. HERE map has vector-based map data, which provides offline capabilities and comes with valuable features, such as navigation, historical traffic patterns, congestion zone maps, real-time traffic, and accidents. In addition, it supports the integration of HERE REST services on mobile devices

displaying raster map tiles and providing an easy way to offer a basic, personalized location experience[48]–[50]. During the trip, the system registers the data whenever there is a change in the data entry, i.e. road name change, traffic severity change, number of lane change, etc. Additionally, the system can detect if the user diverts from the original path and will then re-route him/her to a new path to the destination. (Figure 5) shows some screenshots from the navigation app.

3.2.2 Recommender Component

Upon receiving a request for a route from the Controller, the Recommender component queries the Here Maps API for a list of routes. Each route returned by the Here Maps API is associated with a Travel Time and Congestion Level. The Recommender Component forwards the list of routes to the Stress Predictor to estimate the Stress Level associated with each route. Hence, the Recommender component gathers the following information for each route:

- Travel Time for route i (TTi)
- Congestion Level i (CLi)
- Stress Level for route i (SLi)

In addition, the recommender component obtains the user's preferences from the Preferences Database. We summarize these preferences in four variables:

1. Question Highways (QH): Corresponds to the question presented in (Figure 4a). Its value ranges between 1 and 5, where 1 indicates a strong dislike and 5 strong preference for highways.

2. Question Unfamiliar (QU): Corresponds to the question presented in (Figure 4b). Its value ranges between 1 and 5, where 1 indicates a strong dislike and 5 strong preference for unfamiliar roads.

3. Question Congestion Level routes (QCL): Corresponds to the question presented in (Figure 4c). Its value ranges between 1 and 5, where 1 indicates a strong dislike and 5 strong preference for longer routes that present less congestion.

4. Question Travel Time (QTT): Corresponds to the question presented in (Figure 4d). Its value ranges between 1 and 5, where 1 indicates a strong dislike and 5 strong preference for longer travel times.

For each route, the Recommender component calculates the percentage of the route that is regarded as highway. We define PHi as the percentage of highway road for route i. Moreover, the Recommender calculates PUi as the percentage of unfamiliar road for route i. The Recommender obtains the number of times each road has been travelled along the route from the Preference Database. A road that has been travelled less than two times is considered unfamiliar. Evidently, the system is unaware of the roads travelled before the system was deployed. However, the system would ramp up its knowledge on the roads most frequently travelled by the driver after a few weeks of use to obtain an indication of which roads are most frequently travelled and hence most familiar.

The Recommender component ranks the routes by their travel time, where given N routes, the fastest route is ranked as 1, and the slowest as N. Therefore, we define TTRanki as the rank of route i according to its travel time. Furthermore, the Recommender component ranks the routes by their congestion level, where given N routes, the least congested route is ranked as 1, and the most congested route as N. Therefore, we define CLRanki as the rank of route i according to its length.

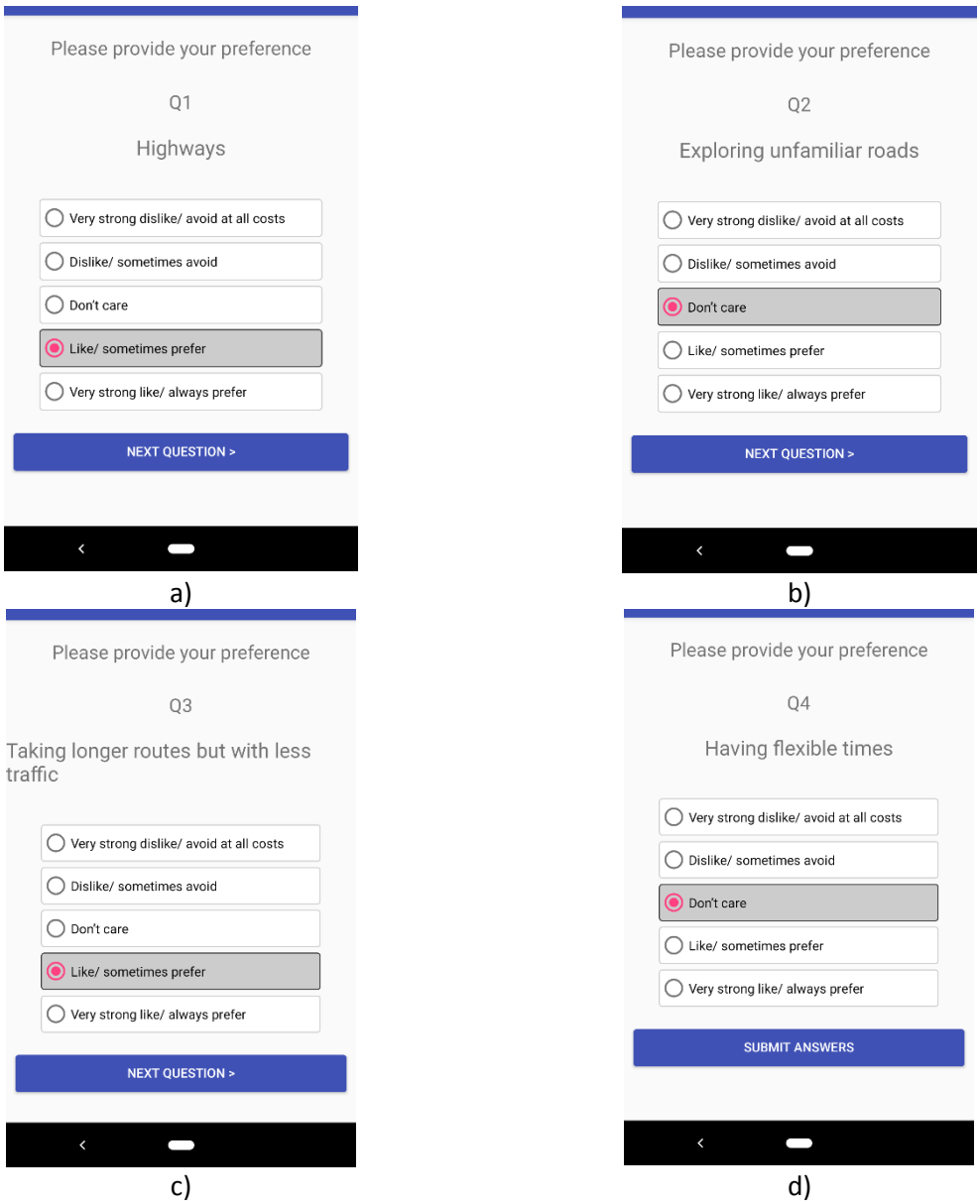

Figure 4: The questioner from which the app will configure the route for the user

The Recommender component calculates a score for each route obtained from the Here Map API using equation (1).

$$score_i = PH_i \times \frac{QH-3}{2} + PU_i \times \frac{QU-3}{2} + \frac{(N+1)-CLRank_i}{N} \times \frac{QCL-3}{2} + \frac{(N+1)-TTRank_i}{N} \times \frac{QTT-3}{2} \quad (1)$$

Where N is the number of routes.

In equation (1), the Likert score for each question is converted into a weight ranging between -1 and 5 to reflect the user's opinion about a preference.

To take the SL variable into account, we further adjust the calculated score for each route using equation (2).

$$stressScore_i = \frac{score_i}{SL_i} \quad (2)$$

The Recommender component returns the route with the highest stressScore as it would be deemed the route that takes into account the user's preferences and predicted stress level.

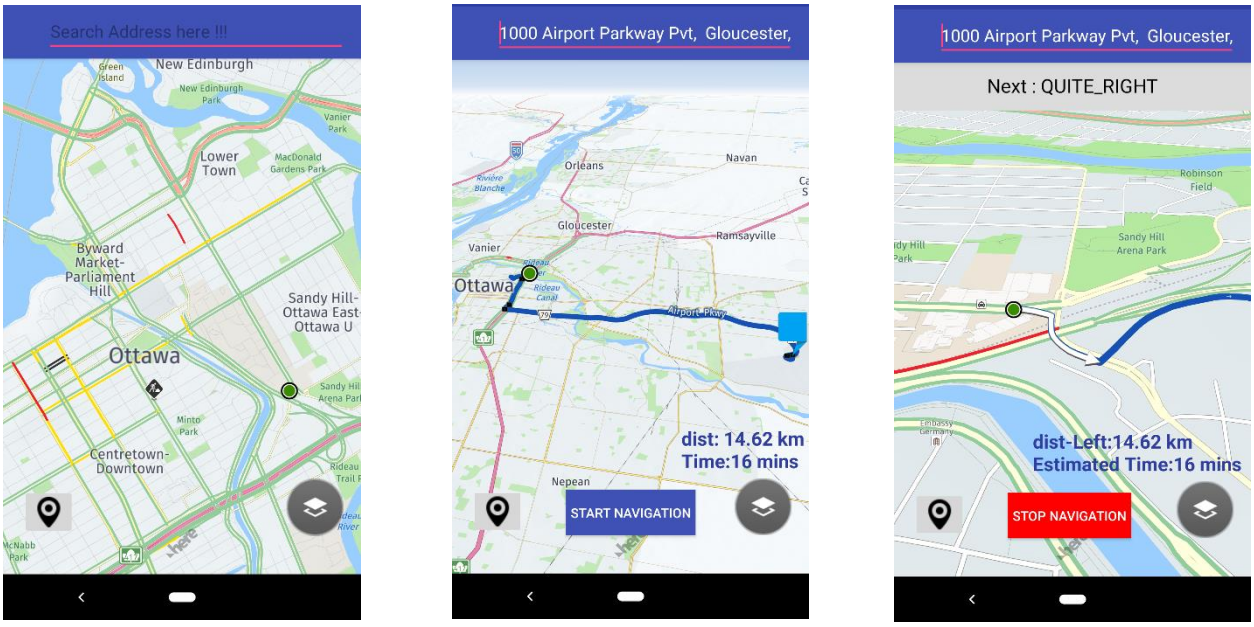

Figure 5: Screenshots from the navigation app

3.1 Stress Detection Setup

An important component of the proposed system is stress prediction. Hence, the system has to collect stress information mapped to road attributes to train a machine-learning model to predict stress. The main goal was to collect the road attributes along with driver's physiological signals conveniently and most importantly "accurately".

To investigate the suitability of the physiological sensor for the type of application we propose, we performed a three-phase investigation. We summarize these phases in the following sections.

Phase1: We took the measurements using a regular Android smartwatch (Misfit Vapor) along with an ECG belt (Bioharness 3) (Figure 6), as a ground-truth measurement tool. The PPG sampling rate from the watch was around 20hz, which is not efficient for HRV calculations. Therefore, we amplified the reading rate to 200hz. However, the data was so susceptible to movement artifacts, especially considering the driver's hand movements while driving, which made the data collected from the watch unusable most of the time.

Figure 6: Zephyr Bioharness sensor [left], Misfit Vapor smartwatch [right]

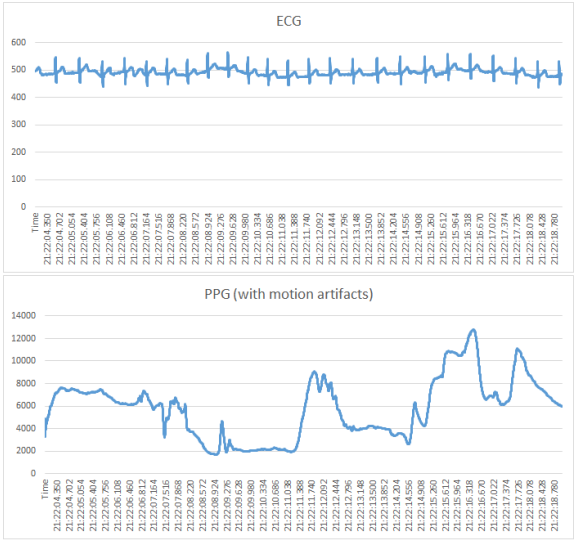

Figure 7: Comparison between ECG and PPG signals

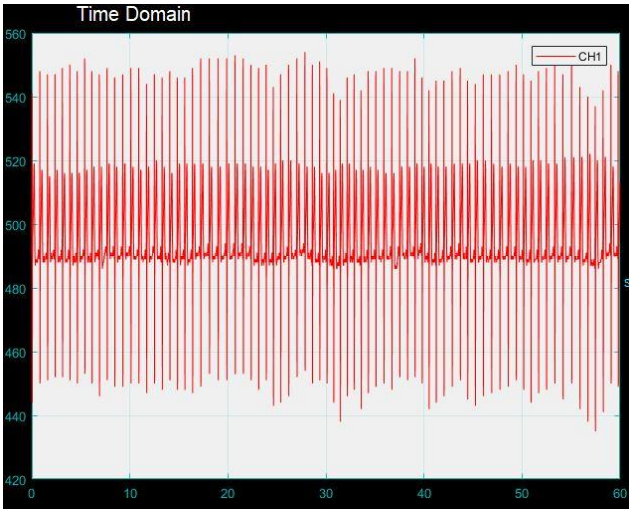

[A] Raw ECG 60sec

[B] Raw PPG 60sec

[C] Raw ECG 10sec

[D] Filtered PPG 10sec

Figure 8: Comparison between RAW/filtered PPG and ECG signals while driving

As seen in (Figure 7 & Figure 8) the ECG signals are much clearer than the PPG signals when it comes to extracting HRV, even when the PPG is filtered. While it is also possible to extract HRV from PPG, it requires many extra steps. It is worth mentioning that PPG signals are prone to motion artifacts, where the noise sometimes replaces the real data when the sensor is misplaced or not in direct contact with the skin. Furthermore, since the data is collected from the driver while he/she is driving, the fact

that the PPG sensor is placed on the wrist makes the data very noisy as both hands need to be on the wheel to properly maneuver the vehicle, thus generating a lot of motion artifacts from the PPG sensor.

Phase2: At this time we switched to a more laboratory focused device, the (Empatica E4) (Figure 9) wristband. It has more accurate sensors and a data filtering mechanism, which uses the gyroscope to eliminate noise from PPG signals. It also generates an Inter Beats Intervals (IBI) file, which is equivalent to R-R (peak to peak time difference), to measure the heart rate variability. However, we concluded that similar to other PPG devices, this one is also susceptible to motion artifacts. When the device detects motion via its gyroscope and accelerometer sensors, it stops recording from the PPG sensor until it is stable for at least 10 seconds. This makes the IBI file unusable since it has large gaps where there were wrist motions. Even worse, when the device detects a lot of movement, there are instances when the IBI file contains no data at all. In the context of our experiment, as there are a lot of hand movements during driving, relying on the PPG sensor to detect stress levels requires many additional steps in order to acquire precise and useful information.

Figure 9: Empatica E4 wristband [side and back]

Figure 10: Polar H10 ECG sensor

Phase3: Finally, we decided to use an ECG belt only, but this time the (Polar H10) belt (Figure 10). ECG is the gold standard in HRV measurement and the device provided a clean signal that we could use to obtain an accurate assessment of stress level.

Since the driver's movements are limited while sitting (compared to other physical activities that can induce stress, such as running, swimming, or even walking), moving the arms, the legs, or turning the head would not significantly increase the stress index. Therefore, the range of the stress index for the driver is theoretically limited as most of the stressors affect the subject mentally.

3.3.1 Window Size and Overlapping

The window size used for HRV measurement is 3 minutes, and the overlap is 30 seconds before the road segment, then a 30-second shift, until the last 30 seconds of the road segment. Finally, the system takes the median stress index of all the windows over that road segment. For example, (Figure 11) shows a path that has four different roads (A, B, C, and D) where road A has three HRV windows (A1, A2, and A3) each window is shifted 30 seconds from the opening of the previous one.

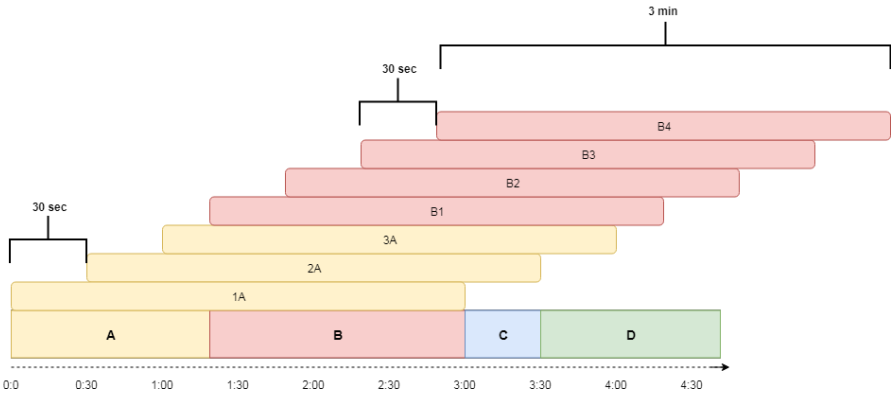

Figure 11: Shifting HRV windows over road segments for smoothing the SI

3.3.2 Stress Index (SI) Smoothing

The stress index also known as Index of Regulatory System Tension. It is calculated using equation (3) from Baevsky [51]

$$SI = \frac{AMo}{2Mo} * MxDMn \qquad (3)$$

- AMo: is the amplitude of a mode which is the number of R-R intervals
- Mo (Mode): the most frequent value occurred in the dynamic range of R-R intervals
- MxDMn: Variation scope which is the difference between Maximal and Minimal value

For each individual, the mean stress index for each road segment (i.e. A, B, C, etc.) is calculated and , consequently, for the whole trip.

3.5 Database Tables

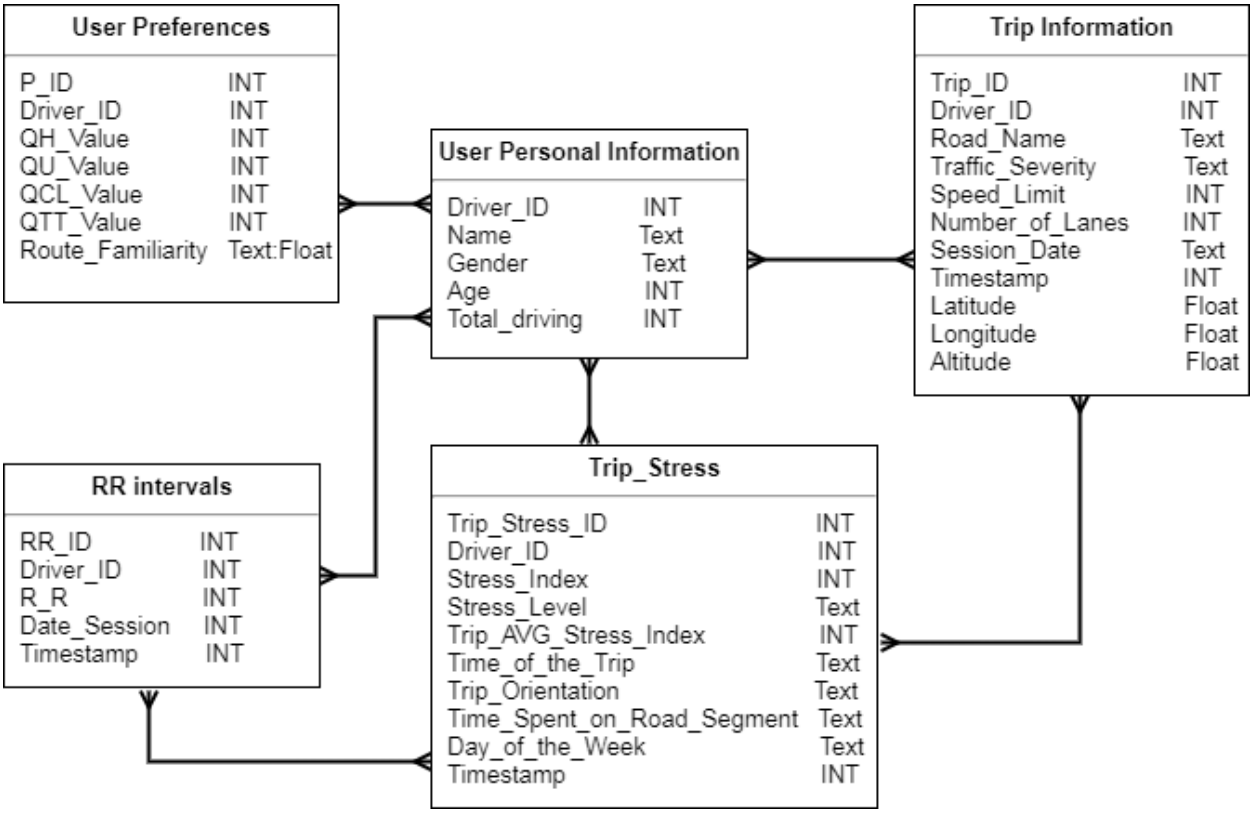

Figure 12: The Entity Relationship Diagram of the system

A. User Information

The driver's personal information database table is shown in Table 3.1 and contains the driver's personal information and total driving time.

Table 3.1: Driver Information

Name	Type	Description
Driver_ID	Integer	A unique identifier for each user
Name	Text	The full name of the user
Gender	Text	The gender of the user
Age	Integer	The age of the user
Total_Driving	Integer	The total amount of driving for the user in minutes

B. User Preferences

During the app setup, the user is asked a few questions that will impact route calculation.

Table 3.2: User Route Preferences

Name	Type	Description
PID	Integer	A unique identifier for each user preferences
Driver_ID	Integer	A unique identifier for each user
QH_Value	Integer	The selected value to highways question
QU_Value	Integer	The selected value to unfamiliarity question
QCL_Value	Integer	The selected value to congestion level question
QTT_Value	Integer	The selected value to travel time question
Route_Familiarity	Text:Float	Route familiarity to the driver (Country-City-Road:value)

C. Trip Information

The collected information during the trip from the navigation app is then stored in the dataset of each driver.

Table 3.3: Trip Information

Name	Type	Description
Trip_ID	Integer	A unique identifier for each trip the driver takes
Driver_ID	Integer	A unique identifier for each user
Road_Name	Text	The name of the road or street
Traffic_Severity	Text	Three levels of traffic severity (Normal, High, Very High)
Speed_Limit	Integer	Speed limit on each road segment
Number_of_Lanes	Integer	Number of lanes on the road
Session_Date	Text	The date of the trip (year-month-day)
Timestamp	Integer	The time when the user takes the road (hour:min:sec)
Latitude	Float	A defined coordinate to specify a location using South–North position points
Longitude	Float	A defined coordinate to specify a location using East-West position points
Altitude	Float	A defined coordinate to specify a location using the Height from sea level

D. Trip R-R Intervals

The data collected from the ECG belt then stored as a file that contains the recorded sessions of the R-R intervals of the driver during the trip and is then exported to the dataset for stress analysis.

Table 3.4: RR Intervals

Name	Type	Description
RR_ID	Integer	A unique identifier for each RR taken of the user
Driver_ID	Integer	A unique identifier for each user
RR	Integer	The value of the RR intervals (ms)
Timestamp	Integer	The time of the first R peak detected during the session (hr:min:sec.ms)
Session_date	Text	The date of the RR intervals session (year-month-day)

E. Trip Stress Data

This table contains the classified trip data concatenated with stress information on each road segment

Table 3.5: Trip Stress

Name	Type	Description
Trip_Stress_ID	Integer	A unique identifier for each trip with driver stress levels
Driver_ID	Integer	A unique identifier for each user
Stress_Index	Integer	The calculated stress index from a 3 min window of HRV on each road segment the driver takes
Stress_Level	Text	Three levels of stress (Low, Normal, High)
Trip_AVG_Stress_Index	Integer	The average stress index during the whole trip
Time_of_the_Trip	Text	Four times of day (morning, afternoon, evening, and night)
Trip_Orientation	Text	The starting point and destination of the trip (Home to Work, Work to Home)
Time_Spent_on_RoadSegment	Text	The time spent by the driver on the same street categorized into (below 1 min, between 1-2 min, between 2-3 min, above 3min)
Day_of_the_Week	Text	Day of the week (Monday - Sunday)
Timestamp	Integer	The time of each road segment (hr:min:sec)

CHAPTER 4. RESULTS, EVALUATION AND DISCUSSION

In this chapter, we summarize our effort to evaluate the stress prediction capacity of the system. Predicting the stress associated with various routes allows the system to make informed decisions regarding routing that take into consideration the stress impact of these routes.

4.1 Data collection

The experiments were performed in real driving conditions, on home-to-work and work-to-home routes. For each subject, the average duration of each trip was 15 minutes, with an average of 12 trips per participant. The equipment used to acquire the needed information was a Polar H10 belt to collect the ECG signals; it was placed on the user's chest before each trip, and an Android phone (Samsung Galaxy S9), which was connected to the ECG sensor via Bluetooth. The developed app allowed us to make a navigation assistant that could save the trip data which contains road segment information during the commute (road name, number of lanes, speed limit, traffic severity, time, and date). As for the stress analysis, the system analyzes HRV data to calculate the average Stress Index (SI) for each road segment, during each trip, for every individual.

4.1.A *Subjects Selection Criteria*

In order to be selected as a driver for this study, individuals first needed to meet the following criteria:

1) Between 20 and 60 years old

2) Have a full G driver's license

3) Lives in the Ottawa-Gatineau area

4) Drives regularly from home to work and vice versa.

Data collection happened over a span of two weeks, for each user. One week involved the navigation guidance and the other week was just about monitoring the trip. At the beginning of the experiment, the user starts the ECG recording. Then, the participant starts the navigation app, which collects the road attributes during the trip. After the end of the trip, the trip app automatically saves the data in the device, and the user stops the HRV collection and enters any additional notes about the road.

The total number of participants in the study was nine (six males and three females), aged between 20 and 42 years old. The driving experience varied from two years up to over twenty years. However, not all drivers were included in the study due to incomplete datasets or missing/corrupt data files, or withdrawal from the study. Thus, making the total number of subjects down to five (four males, and one female). Table 4.1 shows the dataset of the included drivers.

Table 4.1: Participant Dataset

Driver No.	**Total Trips**	**Total Recorded Time (min)**	**Dataset Instances**
Driver01	11	198	117
Driver05	15	215	162
Driver06	12	149	103
Driver07	11	336	116
Driver09	12	204	117
Average	12.20	220.40	124.75
Total	61	1102	615

4.1.B *Context Classification*

To feed the data into an ML model, we clustered the numeric attributes into nominal variables. For example, instead of providing a specific trip time, we classified it into time of day categories, such as morning, night, etc.

Table 4.2: Classification of Trip Attributes

Attribute	Range	Variable
Day of the Week	Date	Monday – Sunday
Trip Time	0:00 – 5:59 6:00 – 11:59 12:00 – 17:59 18:00 – 23:59	Night Morning Afternoon Evening
Time Spent on a Road Segment	1 – 59 sec 60 – 120 sec 121 – 180 sec More than 180 sec	Below 1 min Between 1 – 2 min Between 2 – 3 min Above 3 min
Trip Orientation	Source - Destination	Home-to-Work Work-to-Home
Number of Lanes	1 - 6	Numeric
Speed Limit	10 – 100 km/h	Numeric
Stress Level	Stress index: 1 – 6 7 – 14 More than 15	Low Normal High

We organized the data in an Excel file and then converted it to CVS format in order to import it into the Waikato Environment for Knowledge Analysis (Weka) and save it in an Attribute Relation File Format (ARFF), which is a type of file used for classification and training. Weka offers many classifiers from which we chose 10, namely, Naïve Bayes, Logistic Regression, Multilayer Perceptron, SMO (support-vector machine), IBK, LogitBoost, J48, Random Tree, Decision Stump, JRip and an add-on tool (Auto-WEKA)[52], to compare their outcomes. Weka is Java based and its libraries can be deployed on Android and invoked from Android application.

4.1.C *Algorithms Used for ML*

Naïve Bayes

The Naive Bayes algorithm is a simple probabilistic classifier that calculates a set of probabilities by counting the frequency and combinations of values in a given dataset. Independent attributes are given the value of the class variable. This conditional independence assumption rarely holds true in real-world applications, hence the characterization as naïve. Yet, the algorithm tends to perform well and learn rapidly in various supervised classification problems. This "naivety" allows the algorithm to easily construct classifications out of large datasets without resorting to complicated iterative parameter estimation schemes [53].

Logistic Regression

This technique employs regression to predict the probability of an outcome that can have only two values. One or several predictors are used to make the prediction. Logistic regression produces a logistical curve that is confined to values between 0 and 1. The curve is constructed using the natural logarithm of the odds of the target variable and not the probability [54].

Multilayer Perceptron

The Multi-Layer Perceptron (MLP) is a type of artificial neural network that consists of a nonlinear activation function in the hidden layer. It provides nonlinear mapping between input and output vectors. Neural networks have two important functions i.e. pattern classifiers and nonlinear adaptive filters. A general framework of the neural network consists of three-layer architecture i.e. an input layer that defines the input value, one or more hidden layers that define the mathematical function, and an output layer that defines the final outcome. Each layer consists of a large number of neurons that are interconnected through weights. Each neuron has a mathematical function (also known as an activation function) that accepts inputs from the previous layer and produces outputs for the next layer. So, in neural networks, the prediction is defined by the activation function [55].

SMO

Sequential Minimal Optimization (SMO) is an algorithm used for training Support Vector Machines classifier (SVM), using polynomial or Gaussian kernels. Missing values are replaced globally, nominal attributes are transformed into binary ones, and attributes are normalized by default. One advantage of using this implementation is that the amount of memory required by SMO is linear to the size of the data[56].

IBK

One of the simplest forms of classification algorithms is Nearest Neighbor implementation. IBK is an instance-based learning scheme, depicted as statistical learning algorithms and used for classification. The new item is assigned to the class that is most common amongst its k nearest neighbours. IBK is an implementation of the k-nearest-neighbours classifier. The number of nearest neighbours (k) can be set manually, or determined automatically using cross-validation [57].

LogitBoost

The Weka LogitBoost classifier is based on a well-known AdaBoost procedure. The AdaBoost procedure trains the classifiers on weighted versions of the training samples. It gives a higher weight to those that are misclassified. That part of the procedure is conducted for a sequence of weighted samples. Afterward, the final classifier is defined to be a linear combination of the classifiers from each stage. LogitBoost uses an adaptative Newton algorithm to fit an additive multiple logistic regression model [58].

J48

The J48 algorithm is an implementation of the C4.5 decision tree learner. This implementation produces decision tree models. It recursively splits a dataset according to tests on attribute values in order to separate the possible predictions. The algorithm uses the greedy technique to induce decision trees for classification. A decision-tree model is built by analyzing the training data and the model is used to classify the trained

data. J48 generates decision trees. The node of the J48 decision trees evaluates the existence and the significance of every individual feature [59].

Random Tree

Random Tree is an algorithm used to construct a tree that considers K random features at each node. It performs no pruning. Weka Random Tree generates a full classification for each node [60]. A random tree is a tree drawn at random from a set of possible trees. In this context, ‘‘at random’’ means that each tree in the set of trees has an equal chance of being sampled. Another way of saying this is that the distribution of trees is ‘‘uniform’’. Random trees can be generated efficiently and the combination of large sets of random trees generally leads to accurate models. Random tree models have been extensively developed in the field of Machine Learning in recent years [61].

Decision Stump

A decision stump is a machine-learning model consisting of a one-level decision tree i.e., it is a decision tree with one internal node (the root), which is immediately connected to the terminal nodes (its leaves). A decision stump makes a prediction based on the value of just a single input feature, therefore, they are also called 1-rules [62].

JRip

JRip is an optimized version of IREP[63]. W. Cohen implemented a propositional rule learner, Repeated Incremental Pruning to Produce Error Reduction (RIPPER)[64], in order to increase the accuracy of rules by replacing or revising individual rules. Reduce Error Pruning was used to isolate some data for training and decides when to stop adding more conditions to a rule[65].

4.1.D *Assessment*

The following five different tests and experimental settings were applied to the ECG datasets.

1- 2 Folds: a cross-validation with 2-folds, where the test set and the training set at the same size.

2- 10 Folds: a cross-validation with 10-folds.

3- 70% Split: The dataset was split into two parts, where 70% was used as the training set and the other 30% as the test set.

4- Auto-Weka: a tool that performs a combined algorithm selection and a hyper-parameter optimization over the classification, in Weka, to suggest the best-generalized algorithm.

4.2 Results

Since this approach is for personalized routing, we found that there are stronger correlations with the stress index in the individualized case than in the generalized one. That is, training an ML model for a single user allows it to achieve better predictive accuracy compared to training on the data of a set of users. Stress tends to be a highly personal experience and hence significant differences across members of a population may exist. Therefore, to achieve true personalization of the routing process to minimize mental stress, we must train an ML model for each user that takes into account her/his particularities.

At first glance, the data seems to indicate that road unfamiliarity has a strong relationship with an increased stress index. Then, after a few trips on the same route, the user shows a lower stress value despite almost identical road conditions and travel time. In addition, the stress analysis showed that some drivers have stronger reactions to traffic than others. For these drivers, the correlation between the stress index and the traffic severity is significantly greater than the correlation for other road attributes. For example, in (Figure 13) both drivers have similar road conditions (i.e. traffic severity and trip duration) both have more traffic in trip 1 compared to trip 2, however, driver_1 shows higher stress levels compared to driver_6. In such a case, route planning should focus on avoiding highly congested roads. Interestingly, taking a favourite route showed a reduced stress index compared to other routes,

even when the favourite route was more congested and took longer to arrive at the destination. Thus, familiarity with the road has a significant impact on driver stress.

Figure 13: Stress Comparison between Driver_1 and Driver_6 (Home-to-Work same route)

Another observation is that not all the drivers physiologically respond to road attributes the same way. For example, highly congested roads can induce stress for some drivers, but others show no, or a minimal, increase in stress index when using highly congested roads. In addition, if the high volume of traffic is only in one or two road segments during the trip, and is of short duration, it does not have a substantial impact on driver stress. Therefore, it would not increase the cost value of the suggested route compared to other routes with a theoretically optimum routing (when the stress index is not taken into consideration).

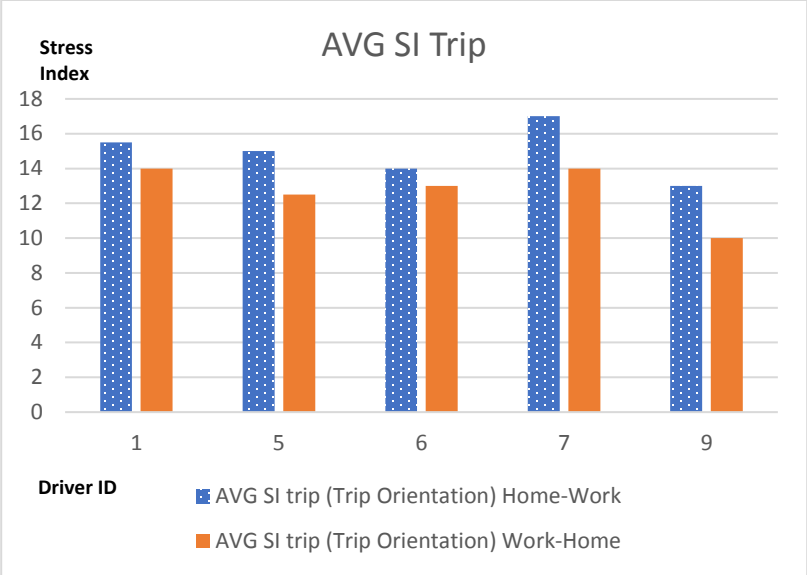

Figure 14: A Comparison between the AVG trip Stress Index based on the trip orientation

There are other factors that play a role in overall stress, such as age and driving experience. The more experienced the driver, with no recent accidents, the lower the overall stress; the lower the experience, the higher the stress. Another common observation was the effect the destination of the trip had on driver stress levels. Most subjects showed higher stress levels during the trip going to work compared to the trip driving back home (Figure 13). This was the case even when the traffic was worse on the way home. The participants were divided into two groups. The first group took their favourite route to work in the first week, and in the second week, they followed the navigation instructions. For the other group, the sequence was reversed; they followed the navigation instructions the first week and took their favourite route the second week. At the end, we excluded the data that was not adequate (i.e. missing or insufficient trip data file). Moreover, we excluded the long stops between trips.

Similar to the approach used in [26] and [42] of exploiting ML to evaluate the system's accuracy, on stage (A) we used seven road features and three classes to predict the stress of each induvial. On stage (B) we used the same features and included (Road Names) in order to examine the stress prediction with

road familiarity for each individual. Using Weka, we show the accuracy, the false positive rate, the precision, recall, and the F-Measure for each participant.

4.2.1 Evaluation Metrics for Stress Level Prediction

In our study, we used the confusion matrix of a 10-fold cross-validation. Consider the ten selected algorithms (*Naïve Bayes, Logistics, Multilayer Perceptron, SMO, IBK, LogitBoost, J48, Random Tree, Decision Stump,* and *JRip*) running on the individual dataset in Weka. We obtained three classes for a 3x3 confusion matrix for each user's dataset. Based on the confusion matrix, we obtained the following well-known evaluation measurements: accuracy, precision, recall, and F-measure. Additionally, the predicted versus the actual (which are the basic measures) are used to evaluate the prediction results. Recall, on one hand, is the measurement that evaluates the predicted level based on only the relevant level in the database, as shown in Formula (3). Precision, on the other hand, is evaluated based on both the total number of irrelevant and relevant level predictions, as shown in Formula (4). Both precision and recall are calculated using each of the TP-FP (5), (6) rates from the confusion matrix. In other words, precision is known as the positive predictive value while recall shows the sensitivity. The trade-off of both precision and recall is the F score (7).

$$Recall = \frac{|\{\text{relevant Stress Level}\} \cap \{\text{predicted Stress Level}\}|}{|\{\text{relevent Stress Level}\}|} \quad (3)$$

$$Precision = \frac{|\{\text{relevant Stress Level}\} \cap \{\text{predicted Stress Level}\}|}{|\{\text{predicted Stress Level}\}|} \quad (4)$$

TP Rate: when the predicted stress level is the same as the actual stress level (the higher the rate the higher the accuracy). (5)

FP Rate: when the predicted stress level is not the same as the actual stress level (the lower the rate the better). (6)

$$F = 2\,\frac{Precision \times Recall}{Percision + Recall} \qquad (7)$$

F-Measure: The trade-off of precision and recall.

The results were divided into two stages: (A) Per Individual Dataset, and (B) Group Dataset

4.2.2 Stage (A): Results of Individual Datasets with Three Classes and Seven Attributes

In the next tables, we present the prediction accuracy of the model (Tables x.x.1), false positive rate (Tables x.x.2), precision rate (Tables x.x.3), recall rate (Tables x.x.4), and f-measure rate (Tables x.x.5). We used ten algorithms [Naïve Bayes, Logistic Regression, Multilayer Perceptron, SMO, IBK, LogitBoost, J48, Random Tree, Decision Stump, JRip as well as an add-on tool (Auto-Weka)] and the classifier it selected with its arguments, to acquire the highest accuracy] and three classification methods (2-folds, 10-folds cross-validation, and 70% data split) with a 3x3 confusion matrix.

The attributes are (Number of Lanes, Speed Limit, Traffic Severity, Trip Time, Time Spent on Each Road Segment, Trip Orientation, and Day of the Week), with three classes for stress level (low, normal, and high).

Driver no. 1

Table 4.1.1 Accuracy Percentage

Classifier	Classification Methods		
	2 folds	10 Folds	70% Split
Naïve Bayes	70.94	70.08	66.66
Logistics	66.66	70.08	66.66
Multilayer Perceptron	66.66	65.81	69.44
SMO	72.64	70.08	69.44
IBK	72.64	65.81	69.44
LogitBoost	70.08	66.66	69.44
J48	71.79	72.64*	72.22
Random Tree	74.35*	64.95	77.77*
DecisionStump	61.53	60.68	66.66
JRip	69.23	70.08	69.44
Auto-WEKA	74.35		

Table 4.1.2 False Positive Rate

Classifier	Classification Methods		
	2 folds	10 Folds	70% Split
Naïve Bayes	0.306	0.309	0.348
Logistics	0.351	0.320	0.354
Multilayer Perceptron	0.336	0.354	0.323
SMO	0.276	0.301	0.329
IBK	0.276	0.335	0.317
LogitBoost	0.312	0.351	0.329
J48	0.291	0.280*	0.292
Random Tree	0.263*	0.342	0.236*
DecisionStump	0.381	0.415	0.360
JRip	0.323	0.316	0.317
Auto-WEKA	0.263		

Table 4.1.3 Precision Rate

Classifier	Classification Methods		
	2 folds	10 Folds	70% Split
Naïve Bayes	0.708	0.700	0.671
Logistics	0.655	0.700	0.681
Multilayer Perceptron	0.669	0.657	0.706
SMO	0.728	0.703	0.723
IBK	0.728	0.666	0.697
LogitBoost	0.700	0.665	0.723
J48	0.717	0.726*	0.730
Random Tree	0.744*	0.659	0.790*
DecisionStump	0.622	0.603	0.700
JRip	0.691	0.699	0.697
Auto-WEKA	0.744		

Table 4.1.4 Recall Rate

Classifier	Classification Methods		
	2 folds	10 Folds	70% Split
Naïve Bayes	0.709	0.701	0.667
Logistics	0.667	0.701	0.667
Multilayer Perceptron	0.667	0.658	0.694
SMO	0.726	0.701	0.694
IBK	0.726	0.658	0.694
LogitBoost	0.701	0.667	0.694
J48	0.718	0.726*	0.722
Random Tree	0.744*	0.650	0.778*
DecisionStump	0.615	0.607	0.667
JRip	0.692	0.701	0.694
Auto-WEKA	0.744		

Table 4.1.5 F-Measure Rate

Classifier	Classification Methods		
	2 folds	10 Folds	70% Split
Naïve Bayes	0.708	0.701	0.660
Logistics	0.664	0.698	0.654
Multilayer Perceptron	0.667	0.657	0.686
SMO	0.727	0.702	0.679
IBK	0.727	0.659	0.691
LogitBoost	0.700	0.664	0.679
J48	0.718	0.726*	0.717
Random Tree	0.744*	0.650	0.774*
DecisionStump	0.617	0.603	0.644
JRip	0.691	0.699	0.691
Auto-WEKA	0.744		

From (Table 4.1.1) the maximum accuracy on the 10-folds is 72.64% and the classifier used to obtain it is *J48*. Using Auto-Weka the accuracy goes to 74.35% by selecting *Random Tree* classifier and the arguments are [-M, 2, -K, 18, -depth, 2, -N, 0]. However, in 2-folds the highest accuracy is 74.35% with the *Random Tree* algorithm. As for the false positive rate (Table 4.1.2), the best results were obtained from the same algorithms with the highest accuracy, specifically, 0.263 using *Random Tree* with 2-folds, 0.280 using *J48* with 10-folds, and 0.236 using *Random Tree* with 70% data split. The highest results for precision, recall, and f-measure (Table 4.1.3, Table 4.1.4, and Table 4.1.5 respectively) were identical with 2-folds and 10-folds (0.744, 0.726 respectively), but it was different with 70% split (0.790, 0.778, and 0.774 respectively).

Driver no. 5

Table 4.2.1 Accuracy Percentage

Classifier	Classification Methods		
	2 folds	10 Folds	70% Split
Naïve Bayes	69.13*	67.9	81.63*
Logistics	64.81	66.66	73.46
Multilayer Perceptron	61.72	64.81	65.3
SMO	66.04	62.96	73.46
IBK	68.51	67.9	69.38
LogitBoost	65.43	64.81	67.34
J48	64.81	67.28	71.42
Random Tree	66.66	70.98*	67.34
DecisionStump	67.28	69.13	73.46
JRip	65.43	64.19	69.38
Auto-WEKA	70.98		

Table 4.2.2 False Positive Rate

Classifier	Classification Methods		
	2 folds	10 Folds	70% Split
Naïve Bayes	0.337	0.354	0.193*
Logistics	0.360	0.366	0.270
Multilayer Perceptron	0.387	0.350	0.337
SMO	0.371	0.429	0.275
IBK	0.332*	0.340	0.311
LogitBoost	0.369	0.387	0.339
J48	0.425	0.345	0.288
Random Tree	0.353	0.306*	0.324
DecisionStump	0.386	0.385	0.290
JRip	0.406	0.392	0.331
Auto-WEKA	0.357		

Table 4.2.3 Precision Rate

Classifier	Classification Methods		
	2 folds	10 Folds	70% Split
Naïve Bayes	0.689*	0.676	0.820*
Logistics	0.650	0.663	0.734
Multilayer Perceptron	0.622	0.655	0.664
SMO	0.657	0.626	0.736
IBK	0.684	0.677	0.693
LogitBoost	0.652	0.644	0.675
J48	0.659	0.671	0.714
Random Tree	0.665	0.709*	0.676
DecisionStump	0.678	0.727	0.766
JRip	0.657	0.638	0.717
Auto-WEKA	0.737		

Table 4.2.4 Recall Rate

Classifier	Classification Methods		
	2 folds	10 Folds	70% Split
Naïve Bayes	0.691*	0.679	0.816*
Logistics	0.648	0.667	0.735
Multilayer Perceptron	0.619	0.648	0.653
SMO	0.660	0.630	0.735
IBK	0.685	0.679	0.694
LogitBoost	0.654	0.648	0.673
J48	0.648	0.673	0.714
Random Tree	0.667	0.710*	0.673
DecisionStump	0.673	0.691	0.735
JRip	0.654	0.642	0.694
Auto-WEKA	0.710		

Table 4.2.5 F-Measure Rate

Classifier	Classification Methods		
	2 folds	10 Folds	70% Split
Naïve Bayes	0.687*	0.674	0.815*
Logistics	0.649	0.661	0.734
Multilayer Perceptron	0.619	0.650	0.652
SMO	0.656	0.610	0.733
IBK	0.684	0.678	0.693
LogitBoost	0.652	0.642	0.670
J48	0.618	0.672	0.714
Random Tree	0.665	0.709*	0.674
DecisionStump	0.655	0.660	0.722
JRip	0.634	0.636	0.679
Auto-WEKA	0.687		

(Table 4.2.1) presents the model prediction accuracy for Driver.5 stress level were the results ranged from 61.72% (with 2-folds using *Multilayer Perceptron*) and up to 81.63% (with 70% split using *Naïve Baye*s). It got even higher using Auto-Weka (96.29%) by selecting *Random Forest* classifier and the arguments are [-I, 18, -K, 0, -depth, 0]. Interestingly in (Table 4.2.2), the best false positive results were from different algorithm in 2-folds than the algorithm with the best accuracy (0.332 with *IBK* vs 0.337 with *Naïve Bayes*). The best precision rate (Table 4.2.3) is 0.820 obtained with 70% split using *Naïve Bayes*. The best results with 10-folds cross validation is 0.709 using *Random Tree* algorithm. As previously, the recall rate (Table 4.2.4) and the f-measure rate (Table 4.2.5) follows the same order of classification methods for the best results (70% split, then 10-folds, then 2-folds).

Driver no. 6

Table 4.3.1 Accuracy Percentage

Classifier	Classification Methods		
	2 folds	10 Folds	70% Split
Naïve Bayes	75.72	79.61	65.62
Logistics	86.40*	82.52	78.12
Multilayer Perceptron	79.61	77.66	75
SMO	82.52	79.61	78.12
IBK	75.72	79.61	78.12
LogitBoost	83.49	79.61	62.5
J48	79.61	75.72	81.25
Random Tree	73.78	79.61	81.25
DecisionStump	79.61	79.61	78.12
JRip	81.55	87.37*	84.37*
Auto-WEKA	89.32		

Table 4.3.2 False Positive Rate

Classifier	Classification Methods		
	2 folds	10 Folds	70% Split
Naïve Bayes	0.588	0.513	0.932
Logistics	0.283*	0.399	0.620
Multilayer Perceptron	0.513	0.518	0.624
SMO	0.505	0.548	0.620
IBK	0.629	0.513	0.620
LogitBoost	0.538	0.548	0.636
J48	0.796	0.700	0.617
Random Tree	0.563	0.442	0.617
DecisionStump	0.796	0.796	0.919
JRip	0.685	0.351*	0.614*
Auto-WEKA	0.382		

Table 4.3.3 Precision Rate

Classifier	Classification Methods		
	2 folds	10 Folds	70% Split
Naïve Bayes	0.744	0.779	0.793
Logistics	0.864*	0.819	0.852
Multilayer Perceptron	0.779	0.765	0.847
SMO	0.807	0.773	0.852
IBK	0.726	0.779	0.852
LogitBoost	0.819	0.773	0.828
J48	N/A	0.703	0.858
Random Tree	0.733	0.793	0.858
DecisionStump	N/A	N/A	0.809
JRip	0.804	0.867*	0.865*
Auto-WEKA	0.896		

Table 4.3.4 Recall Rate

Classifier	Classification Methods		
	2 folds	10 Folds	70% Split
Naïve Bayes	0.757	0.796	0.656
Logistics	0.864*	0.825	0.781
Multilayer Perceptron	0.796	0.777	0.750
SMO	0.825	0.796	0.781
IBK	0.757	0.796	0.781
LogitBoost	0.835	0.796	0.625
J48	0.796	0.757	0.813
Random Tree	0.738	0.796	0.813
DecisionStump	0.796	0.796	0.781
JRip	0.816	0.874*	0.844*
Auto-WEKA	0.893		

Table 4.3.5 F-Measure Rate

Classifier	Classification Methods		
	2 folds	10 Folds	70% Split
Naïve Bayes	0.750	0.785	0.718
Logistics	0.864*	0.822	0.812
Multilayer Perceptron	0.785	0.770	0.791
SMO	0.809	0.780	0.812
IBK	0.738	0.785	0.812
LogitBoost	0.811	0.780	0.702
J48	N/A	0.722	0.833
Random Tree	0.735	0.794	0.833
DecisionStump	N/A	N/A	0.795
JRip	0.761	0.867*	0.854*
Auto-WEKA	0.881		

The results from (Table 4.3.1) shows the best-obtained accuracy (87.37%) with 10-folds using *JRip* algorithm. The second best is 86.40% accuracy with 2-folds using *Logistics*, then comes in third 70% split with 84.37% accuracy using *JRip*. However, with Auto-Weka, the accuracy goes up to 89.32% by selecting *JRip* and the arguments are [-N, 3.1027958855103304, -P, -O, 3]. The best false positive rates from (Table 4.3.2) shows a different order for the classification methods, 2-folds with *Logistics*, then 10-folds with *JRip*, then 70% split also with *JRip* (0.283, 0.351, 0.614 respectively). Precision rate (Table 4.3.3) presents also a different order for best results in classification methods, although it is a

very slight difference, where the highest is 0.867 with 10-folds using JRip, in second is 0.865 with 70% split using JRip, then in third 0.864 with 2-folds using Logistics. Finally, recall and f-measure rates (Table 4.3.4 and Table 4.3.5 respectively) have the same order for best results in classification methods (10-folds with *JRip*, then 2-folds with *Logistics*, then 70% split with *JRip*).

Driver no. 7

Table 4.4.1 Accuracy Percentage

Classifier	Classification Methods		
	2 folds	10 Folds	70% Split
Naïve Bayes	70.69	68.10	75.67
Logistics	66.37	70.68	75.67
Multilayer Perceptron	68.10	66.37	83.78*
SMO	70.68	68.10	54.05
IBK	68.10	65.51	70.27
LogitBoost	69.82	71.55*	75.67
J48	71.55	65.51	64.86
Random Tree	63.79	67.24	64.86
DecisionStump	54.31	62.93	64.86
JRip	75.00*	68.10	78.37
Auto-WEKA	87.06		

Table 4.4.2 False Positive Rate

Classifier	Classification Methods		
	2 folds	10 Folds	70% Split
Naïve Bayes	0.707	0.320	0.272
Logistics	0.356	0.321	0.272
Multilayer Perceptron	0.342	0.349	0.153*
SMO	0.325	0.331	0.462
IBK	0.335	0.363	0.330
LogitBoost	0.335	0.303*	0.251
J48	0.310	0.356	0.409
Random Tree	0.377	0.353	0.388
DecisionStump	0.461	0.442	0.515
JRip	0.268*	0.335	0.211
Auto-WEKA	0.130		

Table 4.4.3 Precision Rate

Classifier	Classification Methods		
	2 folds	10 Folds	70% Split
Naïve Bayes	0.706	0.683	0.755
Logistics	0.662	0.710	0.755
Multilayer Perceptron	0.680	0.662	0.845*
SMO	0.712	0.680	0.556
IBK	0.679	0.653	0.700
LogitBoost	0.704	0.715*	0.760
J48	0.718	0.654	0.641
Random Tree	0.636	0.672	0.645
DecisionStump	0.546	0.677	0.779
JRip	0.751*	0.679	0.792
Auto-WEKA	0.871		

Table 4.4.4 Recall Rate

Classifier	Classification Methods		
	2 folds	10 Folds	70% Split
Naïve Bayes	0.707	0.681	0.757
Logistics	0.664	0.707	0.757
Multilayer Perceptron	0.681	0.664	0.838*
SMO	0.707	0.681	0.541
IBK	0.681	0.655	0.703
LogitBoost	0.698	0.716*	0.757
J48	0.716	0.655	0.649
Random Tree	0.638	0.672	0.649
DecisionStump	0.543	0.629	0.649
JRip	0.750*	0.681	0.784
Auto-WEKA	0.871		

Table 4.4.5 F-Measure Rate

Classifier	Classification Methods		
	2 folds	10 Folds	70% Split
Naïve Bayes	0.706	0.682	0.755
Logistics	0.660	0.700	0.755
Multilayer Perceptron	0.676	0.663	0.839*
SMO	0.699	0.680	0.545
IBK	0.679	0.652	0.701
LogitBoost	0.689	0.713*	0.758
J48	0.710	0.654	0.640
Random Tree	0.636	0.667	0.646
DecisionStump	0.544	0.575	0.554
JRip	0.747*	0.679	0.785
Auto-WEKA	0.871		

In (Table 4.4.1), the best accuracy within the 10-folds is 71.55% using the classifier *LogitBoost* to obtain it, but it is even higher in 70% split at 83.78% accuracy using *Multilayer Perceptron*. Using Auto-Weka, the accuracy goes up to 87.06% by selecting *Random Committee* classifier and the arguments are [-I, 5, -S, 1, -W, weka.classifiers.trees.REPTree, -M, 2, -V, 0.027525727475544194, -L, 18, -P]. As for the false positive rates (Table 4.4.2) the best performance comes from the 70% split (0.153) with *Multilayer Perceptron*. 2-folds classification method comes in second with (0.268) using *JRip*, then 10-folds with (0.303) using *LogitBoost*. Precision, recall, and f-measure rates (Table 4.4.3 , Table 4.4.4, and Table 4.4.5 respectively) have the same order of classification methods and algorithms for the best scores (in first 70% split with *Multilayer Perceptron*, then 2-folds with *JRip*, lastly 10-folds with *LogitBoost*).

Driver no. 9

Table 4.5.1 Accuracy Percentage

Classifier	Classification Methods		
	2 folds	10 Folds	70% Split
Naïve Bayes	82.05	84.61	85.71
Logistics	83.76	90.59	91.42*
Multilayer Perceptron	85.47	89.74	88.57
SMO	82.9	90.59	88.57
IBK	82.9	89.74	88.57
LogitBoost	82.9	89.74	88.57
J48	88.03*	87.17	82.85
Random Tree	85.47	94.87*	88.57
DecisionStump	88.03*	88.03	82.85
JRip	82.9	90.59	88.57
Auto-WEKA	95.72		

Table 4.5.2 False Positive Rate

Classifier	Classification Methods		
	2 folds	10 Folds	70% Split
Naïve Bayes	0.395	0.268*	0.294*
Logistics	0.269	0.383	0.414
Multilayer Perceptron	0.267*	0.384	0.552
SMO	0.270	0.383	0.552
IBK	0.270	0.384	0.552
LogitBoost	0.270	0.384	0.552
J48	0.880	0.882	0.829
Random Tree	0.390	0.377	0.552
DecisionStump	0.880	0.880	0.829
JRip	0.394	0.445	0.552
Auto-WEKA	0.314		

Table 4.5.3 Precision Rate

Classifier	Classification Methods		
	2 folds	10 Folds	70% Split
Naïve Bayes	0.866	0.892	0.867
Logistics	0.890	0.903	0.922*
Multilayer Perceptron	0.895*	0.897	0.900
SMO	0.859	0.910	0.900
IBK	0.888	0.897	0.900
LogitBoost	0.874	0.886	0.900
J48	N/A	0.774	N/A
Random Tree	0.877	0.952*	0.900
DecisionStump	N/A	N/A	N/A
JRip	0.868	0.898	0.900
Auto-WEKA	0.959		

Table 4.5.4 Recall Rate

Classifier	Classification Methods		
	2 folds	10 Folds	70% Split
Naïve Bayes	0.821	0.846	0.857
Logistics	0.838	0.906	0.914*
Multilayer Perceptron	0.855	0.897	0.886
SMO	0.880*	0.915	0.886
IBK	0.829	0.897	0.886
LogitBoost	0.846	0.889	0.886
J48	0.880*	0.872	0.829
Random Tree	0.855	0.949*	0.886
DecisionStump	0.880*	0.880	0.829
JRip	0.829	0.906	0.886
Auto-WEKA	0.957		

Table 4.5.5 F-Measure Rate

Classifier	Classification Methods		
	2 folds	10 Folds	70% Split
Naïve Bayes	0.838	0.862	0.861
Logistics	0.856	0.904	0.902*
Multilayer Perceptron	0.869*	0.897	0.861
SMO	0.849	0.904	0.861
IBK	0.849	0.897	0.861
LogitBoost	0.849	0.897	0.861
J48	N/A	0.820	N/A
Random Tree	0.864	0.942*	0.861
DecisionStump	N/A	N/A	N/A
JRip	0.845	0.901	0.861
Auto-WEKA	0.953		

With Driver.9 we obtained the highest score among all users with a high accuracy of 94.87% using Random Tree with 10-folds cross validation (Table 4.5.1). Interestingly, in 2-folds classification there are two algorithms performed equally the highest (88.03% accuracy) *J48* and *Decision Stump*. Using Auto-Weka, the accuracy goes up to 95.72% by selecting LWL classifier and the arguments are [-K, 30, -A, weka.core.neighboursearch.LinearNNSearch, -W, weka.classifiers.rules.JRip, -N, 3.762806030837358, -P, -O, 4]. However, results on false positive rate shows different classifiers that have the best performance (Table 4.5.2) where *Multilayer Perceptron* in first with 2-folds then *Naïve Bayes* in second with 10-folds and 70% split. In precision rate (Table 4.5.3) *Multilayer Perceptron* performed well at 0.895 in 2-folds, then *Logistics* with 70% split performed better at 0.922, and *Random Tree* has the best score at 0.952 with 10-folds. Even though 2-folds classification in recall rate (Table 4.5.4) does not has the best results compared to other methods, it has three algorithms with the same highest score at 0.880 (SMO, J48, and Decision Stump). Again, 10-folds has the best score among the used classification methods (0.949 with Random Tree). Results in f-measure (Table 4.5.5) shows that *Random Tree* also has the highest score (0.942) in 10-folds compared to 0.902 using *Logistics* in 70% split, and 0.869 using *Multilayer Perceptron* in 2-folds cross validation.

4.2.3 Stage (B): Results on Group Dataset with Three Classes and Seven Attributes

The difference between Stage A and B is that the B dataset contains the entries of *all the users* combined in one group

Table 4.6.1 Accuracy Percentage

Classifier	Classification Methods		
	2 folds	10 Folds	70% Split
Naïve Bayes	62.32	65.33	66.88
Logistics	63.52	67.73	66.88
Multilayer Perceptron	68.13*	71.54*	70.19
SMO	66.33	69.73	70.86*
IBK	65.53	69.94	68.87
LogitBoost	64.73	66.73	67.55
J48	62.52	70.94	68.21
Random Tree	63.12	68.13	66.22
DecisionStump	61.52	61.52	62.91
JRip	62.32	71.34	70.86*
Auto-WEKA	91.18		

Table 4.6.2 False Positive Rate

Classifier	Classification Methods		
	2 folds	10 Folds	70% Split
Naïve Bayes	0.629	0.373	0.356
Logistics	0.435	0.407	0.430
Multilayer Perceptron	0.373	0.322*	0.352
SMO	0.408	0.402	0.406
IBK	0.350*	0.327	0.330
LogitBoost	0.463	0.423	0.411
J48	0.429	0.330	0.327*
Random Tree	0.375	0.348	0.382
DecisionStump	0.615	0.615	0.629
JRip	0.454	0.361	0.370
Auto-WEKA	0.110		

Table 4.6.3 Precision Rate

Classifier	Classification Methods		
	2 folds	10 Folds	70% Split
Naïve Bayes	0.629	0.658	0.677
Logistics	0.626	0.668	0.656
Multilayer Perceptron	0.676*	0.714*	0.699
SMO	0.655	0.691	0.701*
IBK	0.669	0.702	0.698
LogitBoost	0.632	0.656	0.665
J48	0.621	0.708	0.696
Random Tree	0.646	0.684	0.664
DecisionStump	N/A	N/A	N/A
JRip	0.612	0.707	0.701*
Auto-WEKA	0.912		

Table 4.6.4 Recall Rate

Classifier	Classification Methods		
	2 folds	10 Folds	70% Split
Naïve Bayes	0.623	0.653	0.669
Logistics	0.635	0.677	0.669
Multilayer Perceptron	0.681*	0.715*	0.702
SMO	0.663	0.697	0.709*
IBK	0.655	0.699	0.689
LogitBoost	0.647	0.667	0.675
J48	0.625	0.709	0.682
Random Tree	0.631	0.681	0.662
DecisionStump	0.615	0.615	0.629
JRip	0.623	0.713	0.709*
Auto-WEKA	0.912		

Table 4.6.5 F-Measure Rate

Classifier	Classification Methods		
	2 folds	10 Folds	70% Split
Naïve Bayes	0.626	0.655	0.672
Logistics	0.628	0.666	0.657
Multilayer Perceptron	0.678*	0.715*	0.700
SMO	0.656	0.680	0.691
IBK	0.659	0.700	0.692
LogitBoost	0.625	0.654	0.667
J48	0.623	0.708	0.686
Random Tree	0.636	0.682	0.663
DecisionStump	N/A	N/A	N/A
JRip	0.614	0.705	0.702*
Auto-WEKA	0.911		

From (Table 4.6.1) the highest accuracy achieved on the group dataset was 71.54% in 10-folds with *Multilayer Perceptron* algorithm. Nevertheless, using Auto-Weka, the accuracy goes up to 91.18% by

selecting *Bagging* classifier and the arguments are [-P, 81, -I, 93, -S, 1, -W, weka.classifiers.trees.LMT, -M, 4, -W, 0.07789206391602876]. Results on false positive rate (Table 4.6.2) shows that *Multilayer Perceptron* has the best overall score (0.322) with 10-folds cross-validation. Similarly, in precision, recall, and f-measure rates (Table 4.6.3, Table 4.6.4, and Table 4.6.5 respectively) *Multilayer Perceptron* obtained the highest scores with 2-folds and 10-folds classifications.

In all the tables presented previously, the data with * shows the best possible result among the selected algorithms within the same classification method (excluding Auto-WEKA).

Not surprisingly, stress impact factors differ from one person to another, and the more insight we gain about a trip, the more accurately we can determine the reasons for the stress. For example, driving to work late during rush hour has more influence on stress levels than driving back home late at night. For people, driving in unclear weather conditions has a large impact on their stress level; for example, driving through a snowstorm is more stressful than driving on dry roads on a sunny day.

Table 4.6: Stress Level Model Accuracy

Driver_ID	Logistics	JRip	Random Tree	Logit Boost	SMO	Naïve Bayes	IBK	J48	Multilayer Perceptron	Decision Stump	MAX	Algorithm
1	70.08%	70.08%	64.95%	66.66%	70.08%	70.08%	65.81%	72.64%	65.81%	60.68%	72.64%	J48
5	66.66%	64.19%	70.98%	64.81%	62.96%	67.90%	67.90%	67.28%	64.81%	69.13%	70.98%	Random Tree
6	82.52%	87.37%	79.61%	79.61%	79.61%	79.61%	79.61%	75.72%	77.66%	79.61%	87.37%	JRip
7	70.68%	68.10%	67.24%	71.55%	68.10%	68.10%	65.51%	65.51%	66.37%	62.93%	71.55%	Logit Boost
9	90.59%	90.59%	94.87%	89.74%	90.59%	84.61%	89.74%	87.17%	89.74%	88.03%	94.87%	Random Tree
Average	76.11%	76.07%	75.53%	74.47%	74.27%	74.06%	73.71%	73.66%	72.88%	72.08%		
Max	90.59%	90.59%	94.87%	89.74%	90.59%	84.61%	89.74%	87.17%	89.74%	88.03%		

Running each user's dataset through all the pre-selected ML algorithms using 10-Folds cross validation we got the prediction accuracy of the model (Table 4.6) ordered by the highest average. From the previous table, we can observe that there is no algorithm that has the highest accuracy across all the subjects. However, Random Tree has the highest prediction accuracy between two subjects.

Table 4.7: Stress Level Model Accuracy with Logistics regression

Driver ID	Prediction Accuracy
1	70.08%
5	66.66%
6	82.52%
7	70.68%
9	90.59%
Average	76.11%

Although there is no common algorithm to obtain the highest accuracy for all users, the *Logistics regression* is the one that has the highest average accuracy among individual dataset. From the above (Table 4.7), we present the stress level prediction average accuracy achieved using *Logistics regression* in 10-folds cross-validation.

Chapter 5. Conclusion and Future Work

5.1 Conclusion

Although the most influential stressors for a driver could be external factors, such as other drivers, our system focuses on the stress correlated with road attributes and driver road preferences. We Introduced a novel approach by linking road attributes with driver stress levels then using machine learning to predict the stress level of the trip as another measurement alongside time and distance.

Indeed, other drivers could influence the user's stress more than any other stressors, but that is out of the scope of this study. However, we provided an approach to predicting the individual's stress based on previously recorded physiological signals combined with road attributes. Our evaluation results show that our proposed system is able to predict the stress level of the driver with an average accuracy of 76.11%.

Interestingly, a common observation in this study is that when individuals take their favourite path to a destination, they show less overall stress than when they take an unfamiliar path to the same destination; this is true even if that unfamiliar path is considered the optimal route at that time, according to the GPS system.

5.2 Limitations and Future Work

Although it took four months to collect the data from all of the drivers in the field study, the span period for each subject (two weeks) was considerably short for deep learning process. which leaves a room for improvement to increase the system accuracy when collecting a wider scale of data.

With rapidly advancing technology, sensors could detect the physiological signals unobtrusively, for example with a front-facing camera. Thus, making the data collection much easier and more consistent. In addition, this system could be applicable to self-driving vehicles. For example, the user profile has all the road preferences that the driver (in this case the main passenger) prefers. Accordingly, whenever he/she uses a commuting service, the profile carries all of the preferences and stress information regarding road characteristics. Ultimately, when the routing system takes all this information into consideration, it should make the trip less stressful for the passenger.

REFERENCES

[1] E. Gulian, A. I. Glendon, G. Matthews, D. R. Davies, and L. M. Debney, "The stress of driving: A diary study.," *Work Stress*, vol. 4, no. 1, pp. 7–16, 1990.

[2] S. M. Nesbit, J. C. Conger, and A. J. Conger, "A quantitative review of the relationship between anger and aggressive driving," *Aggress. Violent Behav.*, vol. 12, no. 2, pp. 156–176, 2007.

[3] D. J. Bumgarner, J. R. Webb, and C. S. Dula, "Forgiveness and adverse driving outcomes within the past five years: Driving anger, driving anger expression, and aggressive driving behaviors as mediators," *Transp. Res. Part F Traffic Psychol. Behav.*, vol. 42, pp. 317–331, 2016.

[4] G. Matthews, L. Dorn, and A. Ian Glendon, "Personality correlates of driver stress," *Pers. Individ. Dif.*, vol. 12, no. 6, pp. 535–549, 1991.

[5] M. V. Martinez, I. Del Campo, J. Echanobe, and K. Basterretxea, "Driving Behavior Signals and Machine Learning: A Personalized Driver Assistance System," *IEEE Conf. Intell. Transp. Syst. Proceedings, ITSC*, vol. 2015-Octob, pp. 2933–2940, 2015.

[6] J. L. Adler and V. J. Blue, "Toward the design of intelligent traveler information systems," *Transp. Res. Part C Emerg. Technol.*, vol. 6, no. 3, pp. 157–172, 1998.

[7] I. K. and K. B. K. Park, M. Bell, "Learning user preferences of route choice behaviour for adaptive route guidance," *Transp. Res.*, 2007.

[8] J. Letchner, J. Krumm, and E. Horvitz, "Trip router with individualized preferences (trip): Incorporating personalization into route planning," *Proc. Natl. Conf. Artif. Intell.*, vol. 21, no. 2, p. 1795, 2006.

[9] A. H. Taylor and L. Dorn, "STRESS, FATIGUE, HEALTH, AND RISK OF ROAD TRAFFIC ACCIDENTS AMONG PROFESSIONAL DRIVERS: The Contribution of Physical Inactivity," *Annu. Rev. Public Heal.*, vol. 27, no. 16, pp. 371–91, 2006.

[10] G. Matthews, L. Dorn, T. W. Hoyes, D. R. Davies, a I. Glendon, and R. G. Taylor, "Driver stress and performance on a driving simulator.," *Hum. Factors*, vol. 40, no. 1, pp. 136–149, 1998.

[11] G. Rebolledo-Mendez, A. Reyes, S. Paszkowicz, M. C. Domingo, and L. Skrypchuk, "Developing a body sensor network to detect emotions during driving," *IEEE Trans. Intell. Transp. Syst.*, vol. 15, no. 4, pp. 1850–1854, 2014.

[12] J. Healey and R. Picard, "SmartCar: detecting driver stress," *Proc. 15th Int. Conf. Pattern Recognition. ICPR-2000*, vol. 4, pp. 218–221, 2000.

[13] M. Havlikova and S. Sediva, "Monitoring of driver's fatigue - Statistical analysis of test driver trajectories in various environments and in different driver stress degrees," *IFAC Proc. Vol.*, vol. 11, no. PART 1, pp. 146–150, 2012.

[14] S. Vitabile, A. de Paola, and F. Sorbello, "A real-time non-intrusive FPGA-based drowsiness detection system," *J. Ambient Intell. Humaniz. Comput.*, vol. 2, no. 4, pp. 251–262, 2011.

[15] J. a Healey, R. W. Picard, and A. C. Smith, "Wearable and Automotive Systems for Affect Recognition from Physiology Accepted by Wearable and Automotive Systems for A ect

Recognition by," p. 158, 2000.

[16] D. Wiesenthal and D. Hennessy, "Traffic Congestion, Driver Stress, and Driver Aggression," vol. 2337, no. April, 2012.

[17] S. . Westerman and D. Haigney, "Individual differences in driver stress, error and violation," *Pers. Individ. Dif.*, vol. 29, no. 5, pp. 981–998, 2000.

[18] J. D. Hill and L. N. Boyle, "Driver stress as influenced by driving maneuvers and roadway conditions," *Transp. Res. Part F Traffic Psychol. Behav.*, vol. 10, no. 3, pp. 177–186, 2007.

[19] P. J. Legree, T. S. Heffner, J. Psotka, D. E. Martin, and G. J. Medsker, "Traffic crash involvement: Experiential driving knowledge and stressful contextual antecedents," *J. Appl. Psychol.*, vol. 88, no. 1, pp. 15–26, 2003.

[20] I. C. Jeong, D. H. Lee, S. W. Park, J. Il Ko, and H. R. Yoon, "Automobile driver's stress index provision system that utilizes electrocardiogram," *2007 IEEE Intell. Veh. Symp.*, pp. 652–656, 2007.

[21] J. A. Healey and R. W. Picard, "Detecting stress during real-world driving tasks using physiological sensors," *IEEE Trans. Intell. Transp. Syst.*, vol. 6, no. 2, pp. 156–166, 2005.

[22] Y. Hlotova, O. Cats, and S. Meijer, "Measuring Bus Driver ' s Occupational Stress under Changing Working Conditions," *Transp. Res. Board 93rd Annu. Meet. January 12-16, Washington, D.C.*, pp. 13–20, 2014.

[23] H. SELYE, "Forty years of stress research: principal remaining problems and misconceptions," vol. 115, no. July, p. 4, 1976.

[24] _Gary_D._James Gillian_H._Ice, "Measuring Stress in Humans: A Practical Guide for the Field," *Cambridge Univ. Press*, p. 271, 2007.

[25] J. Taelman, S. Vandeput, A. Spaepen, and S. Van Huffel, "Influence of Mental Stress on Heart Rate and Heart Rate Variability," vol. 37, no. January 2016, 2009.

[26] R. A. Alharthi, "Context – Aware Stress Prediction System," 2016.

[27] H. Al Osman, M. Eid, and A. El Saddik, "U-biofeedback: A multimedia-based reference model for ubiquitous biofeedback systems," *Multimed. Tools Appl.*, vol. 72, no. 3, pp. 3143–3168, 2014.

[28] J. Yuan, Y. Zheng, X. Xie, and G. Sun, "T-drive: Enhancing driving directions with taxi drivers' intelligence," *IEEE Trans. Knowl. Data Eng.*, vol. 25, no. 1, pp. 220–232, 2013.

[29] T. Liebig, N. Piatkowski, C. Bockermann, and K. Morik, "Predictive Trip Planning – Smart Routing in Smart Cities," *EDBT/ICDT Work.*, no. c, pp. 331–338, 2014.

[30] H. Mølgaard, K. Hermansen, and P. Bjerregaard, "Spectral components of short-term RR interval variability in healthy subjects and effects of risk factors," *Eur. Heart J.*, vol. 15, no. 9, pp. 1174–1183, 1994.

[31] D. Liao *et al.*, "Age, race, and sex differences in autonomic cardiac function measured by spectral analysis of heart rate variability-The ARIC study," *Am. J. Cardiol.*, vol. 76, no. 12, pp. 906–912, 1995.

[32] S. M. Ryan, A. L. Goldberger, S. M. Pincus, J. Mietus, and L. A. Lipsitz, "Gender- and age-related

differences in heart rate dynamics: Are women more complex than men?," *J. Am. Coll. Cardiol.*, vol. 24, no. 7, pp. 1700–1707, 1994.

[33] H. M. Amar, N. M. Drawil, and O. A. Basir, "Traveler Centric Trip Planning: A Behavioral-Driven System," *IEEE Trans. Intell. Transp. Syst.*, vol. 17, no. 6, pp. 1521–1537, 2016.

[34] A. Hadjali, A. Mokhtari, and O. Pivert, "Expressing and processing complex preferences in route planning queries: Towards a fuzzy-set-based approach," *Fuzzy Sets Syst.*, vol. 196, pp. 82–104, 2012.

[35] A. Mokhtari, O. Pivert, A. Hadjali, and P. Bosc, "Towards a route planner capable of dealing with complex bipolar preferences," *IEEE Conf. Intell. Transp. Syst. Proceedings, ITSC*, pp. 556–561, 2009.

[36] H. Dia, "An agent-based approach to modelling driver route choice behaviour under the influence of real-time information," *Transp. Res. Part C Emerg. Technol.*, vol. 10, pp. 331–349, 2002.

[37] B. D. Ziebart, A. L. Maas, A. K. Dey, and J. A. Bagnell, "Navigate like a cabbie: Probabilistic reasoning from observed context-aware behavior," *10Th Int. Conf. Ubiquitous Comput.*, pp. 322–331, 2008.

[38] D. Papinski, D. M. Scott, and S. T. Doherty, "Exploring the route choice decision-making process: A comparison of planned and observed routes obtained using person-based GPS," *Transp. Res. Part F Traffic Psychol. Behav.*, vol. 12, no. 4, pp. 347–358, 2009.

[39] G. Rigas, Y. Goletsis, and D. I. Fotiadis, "Real-time driver's stress event detection," *IEEE Trans. Intell. Transp. Syst.*, vol. 13, no. 1, pp. 221–234, 2012.

[40] Q. Ji, Z. Zhu, and P. Lan, "Real-time nonintrusive monitoring and prediction of driver fatigue," *IEEE Trans. Veh. Technol.*, vol. 53, no. 4, pp. 1052–1068, 2004.

[41] S. Vhaduri, A. Ali, M. Sharmin, K. Hovsepian, and S. Kumar, "Estimating Drivers' Stress from GPS Traces," *Proc. 6th Int. Conf. Automot. User Interfaces Interact. Veh. Appl. - AutomotiveUI '14*, pp. 1–8, 2014.

[42] N. Keshan, P. V. Parimi, and I. Bichindaritz, "Machine learning for stress detection from ECG signals in automobile drivers," *Proc. - 2015 IEEE Int. Conf. Big Data, IEEE Big Data 2015*, pp. 2661–2669, 2015.

[43] S. Begum, "Intelligent driver monitoring systems based on physiological sensor signals: A review," *IEEE Conf. Intell. Transp. Syst. Proceedings, ITSC*, no. Itsc, pp. 282–289, 2013.

[44] M. Lemay *et al.*, "Wrist:Located Optical Device for Atrial Fibrillation Screening: a Clinical Study on Twenty Patients," pp. 681–684, 2016.

[45] A. Alwosheel, A. Alasaad, and A. Alqaraawi, "Heart rate variability estimation in photoplethysmography signals using Bayesian learning approach," *Healthc. Technol. Lett.*, vol. 3, no. 2, pp. 136–142, 2016.

[46] G. Li and W.-Y. Chung, "Detection of Driver Drowsiness Using Wavelet Analysis of Heart Rate Variability and a Support Vector Machine Classifier," *Sensors*, vol. 13, no. 12, pp. 16494–16511, 2013.

[47] V. Jeyhani, S. Mahdiani, M. Peltokangas, and A. Vehkaoja, "Comparison of HRV parameters

derived from photoplethysmography and electrocardiography signals," *Proc. Annu. Int. Conf. IEEE Eng. Med. Biol. Soc. EMBS*, vol. 2015-Novem, pp. 5952–5955, 2015.

[48] HERE, "HERE maps SDK for Android." [Online]. Available: https://developer.here.com/documentation/android-premium/dev_guide/topics/use-cases.html. [Accessed: 29-Jul-2019].

[49] P. E. Version, "HERE Android SDK Developer ' s Guide Important Information Notices."

[50] P. E. Version, "HERE Android SDK Release Notes Important Information Notices."

[51] R. M. Baevsky and A. P. Berseneva, "Methodical recommendations USE KARDiVAR SYSTEM FOR DETERMINATION OF THE STRESS LEVEL AND ESTIMATION OF THE BODY Standards of measurements and physiological interpretation," 2008.

[52] L. Kotthoff, C. Thornton, H. H. Hoos, F. Hutter, and K. Leyton-Brown, "Auto-WEKA: Automatic Model Selection and Hyperparameter Optimization in WEKA," pp. 81–95, 2019.

[53] G. Dimitoglou, J. A. Adams, and C. M. Jim, "Comparison of the C4 . 5 and a Naive Bayes Classifier for the Prediction of Lung Cancer Survivability," pp. 1–9, 2006.

[54] S. Choudhury and A. Bhowal, "Comparative analysis of machine learning algorithms along with classifiers for network intrusion detection," *2015 Int. Conf. Smart Technol. Manag. Comput. Commun. Control. Energy Mater. ICSTM 2015 - Proc.*, no. May, pp. 89–95, 2015.

[55] Y. kumar and G. Sahoo, "Analysis of Parametric & Non Parametric Classifiers for Classification Technique using WEKA," *Int. J. Inf. Technol. Comput. Sci.*, vol. 4, no. 7, pp. 43–49, 2012.

[56] A. H. Wahbeh and M. Al-Kabi, "Comparative Assessment of the Performance of Three WEKA Text Classifiers Applied to Arabic Text," *Abhath Al-yarmouk "Basic Sci. Eng.,"* vol. Vol. 21, no. 1, pp. 15–28, 2012.

[57] N. Mallios, E. Papageorgiou, M. Samarinas, and K. Skriapas, "Comparison of machine learning techniques using the WEKA environment for prostate cancer therapy plan," *Proc. 2011 20th IEEE Int. Work. Enabling Technol. Infrastruct. Collab. Enterp. WETICE 2011*, pp. 151–155, 2011.

[58] R. W. B Ziolko, S Manandhar, "LOGITBOOST WEKA CLASSIFIER SPEECH SEGMENTATION," *Sci. Technol.*, no. 3, pp. 1297–1300, 2008.

[59] Meenakshi Garg and Kiran Joshi, "Machine Learning Approach for Feature Classification Using Supervised Learning Algorithms," *Natl. J. Adv. Comput.*, vol. 2, no. 1, pp. 247–250, 2011.

[60] A. V. Solanki, "Data Mining Techniques Using WEKA classification for Sickle Cell Disease," *Int. J. Comput. Sci. Inf. Technol.*, vol. 5, no. 4, pp. 5857–5860, 2014.

[61] Y. Zhao and Y. Zhang, "Comparison of decision tree methods for finding active objects," *Adv. Sp. Res.*, vol. 41, no. 12, pp. 1955–1959, 2008.

[62] P. Sharma, "Comparative Analysis of Various Decision Tree Classification Algorithms using WEKA," pp. 684–690.

[63] S. Waseem, A. Salman, and A. K. Muhammad, "Feature subset selection using association rule mining and JRip classifier," *Int. J. Phys. Sci.*, vol. 8, no. 18, pp. 885–896, 2013.

[64] W. W.Cohen, "Fast effective rule induction," vol. 2435.

[65] W. N. H. W. Mohamed, M. N. M. Salleh, and A. H. Omar, “A comparative study of Reduced Error Pruning method in decision tree algorithms,” *Proc. - 2012 IEEE Int. Conf. Control Syst. Comput. Eng. ICCSCE 2012*, pp. 392–397, 2013.

APPENDIX

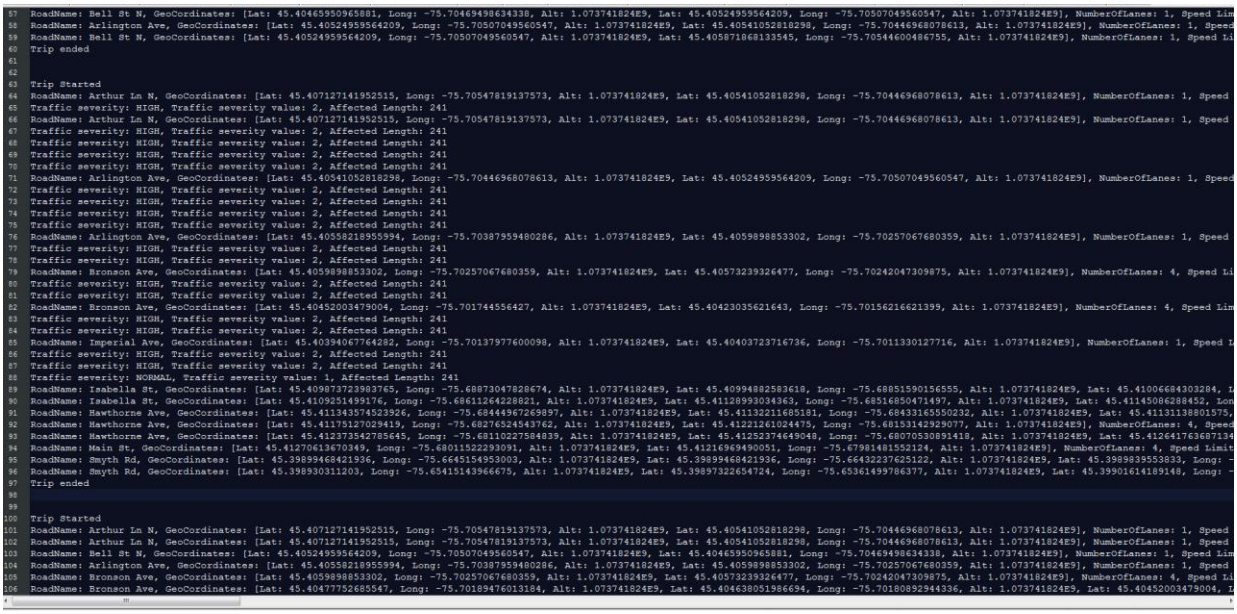

```
RoadName: Bell St N, GeoCordinates: [Lat: 45.40465950965881, Long: -75.70469498634338, Alt: 1.073741824E9, Lat: 45.40524959564209, Long: -75.70507049560547, Alt: 1.073741824E9], NumberOfLanes: 1, Speed Lim
RoadName: Arlington Ave, GeoCordinates: [Lat: 45.40524959564209, Long: -75.70507049560547, Alt: 1.073741824E9, Lat: 45.40541052818298, Long: -75.70446968078613, Alt: 1.073741824E9], NumberOfLanes: 1, Speed
RoadName: Bell St N, GeoCordinates: [Lat: 45.40524959564209, Long: -75.70507049560547, Alt: 1.073741824E9, Lat: 45.40587106133545, Long: -75.70544600486755, Alt: 1.073741824E9], NumberOfLanes: 1, Speed Li
Trip ended


Trip Started
RoadName: Arthur Ln N, GeoCordinates: [Lat: 45.407127141952515, Long: -75.70547819137573, Alt: 1.073741824E9, Lat: 45.40541052818298, Long: -75.70446968078613, Alt: 1.073741824E9], NumberOfLanes: 1, Speed
Traffic severity: HIGH, Traffic severity value: 2, Affected Length: 241
RoadName: Arthur Ln N, GeoCordinates: [Lat: 45.407127141952515, Long: -75.70547819137573, Alt: 1.073741824E9, Lat: 45.40541052818298, Long: -75.70446968078613, Alt: 1.073741824E9], NumberOfLanes: 1, Speed
Traffic severity: HIGH, Traffic severity value: 2, Affected Length: 241
Traffic severity: HIGH, Traffic severity value: 2, Affected Length: 241
Traffic severity: HIGH, Traffic severity value: 2, Affected Length: 241
Traffic severity: HIGH, Traffic severity value: 2, Affected Length: 241
RoadName: Arlington Ave, GeoCordinates: [Lat: 45.40541052818298, Long: -75.70446968078613, Alt: 1.073741824E9, Lat: 45.40524959564209, Long: -75.70507049560547, Alt: 1.073741824E9], NumberOfLanes: 1, Speed
Traffic severity: HIGH, Traffic severity value: 2, Affected Length: 241
Traffic severity: HIGH, Traffic severity value: 2, Affected Length: 241
Traffic severity: HIGH, Traffic severity value: 2, Affected Length: 241
Traffic severity: HIGH, Traffic severity value: 2, Affected Length: 241
RoadName: Arlington Ave, GeoCordinates: [Lat: 45.40558218955994, Long: -75.70387959480286, Alt: 1.073741824E9, Lat: 45.4059898853302, Long: -75.70257067680359, Alt: 1.073741824E9], NumberOfLanes: 1, Speed
Traffic severity: HIGH, Traffic severity value: 2, Affected Length: 241
Traffic severity: HIGH, Traffic severity value: 2, Affected Length: 241
RoadName: Bronson Ave, GeoCordinates: [Lat: 45.4059898853302, Long: -75.70257067680359, Alt: 1.073741824E9, Lat: 45.40573239326477, Long: -75.70242047309875, Alt: 1.073741824E9], NumberOfLanes: 4, Speed Li
Traffic severity: HIGH, Traffic severity value: 2, Affected Length: 241
Traffic severity: HIGH, Traffic severity value: 2, Affected Length: 241
RoadName: Bronson Ave, GeoCordinates: [Lat: 45.404520034790004, Long: -75.701744556427, Alt: 1.073741824E9, Lat: 45.40423035621643, Long: -75.70156216621399, Alt: 1.073741824E9], NumberOfLanes: 4, Speed Lim
Traffic severity: HIGH, Traffic severity value: 2, Affected Length: 241
Traffic severity: HIGH, Traffic severity value: 2, Affected Length: 241
RoadName: Imperial Ave, GeoCordinates: [Lat: 45.40394067764282, Long: -75.70137977600098, Alt: 1.073741824E9, Lat: 45.40403723716736, Long: -75.7011330127716, Alt: 1.073741824E9], NumberOfLanes: 1, Speed L
Traffic severity: HIGH, Traffic severity value: 2, Affected Length: 241
Traffic severity: HIGH, Traffic severity value: 2, Affected Length: 241
Traffic severity: NORMAL, Traffic severity value: 1, Affected Length: 241
RoadName: Isabella St, GeoCordinates: [Lat: 45.40987372398765, Long: -75.68873047828674, Alt: 1.073741824E9, Lat: 45.4094882583618, Long: -75.68051590156555, Alt: 1.073741824E9, Lat: 45.41006684303284, L
RoadName: Isabella St, GeoCordinates: [Lat: 45.4109251499176, Long: -75.68611264228821, Alt: 1.073741824E9, Lat: 45.41128993034363, Long: -75.68516850471497, Alt: 1.073741824E9, Lat: 45.41145086288452, Lon
RoadName: Hawthorne Ave, GeoCordinates: [Lat: 45.411343574523926, Long: -75.68444967269897, Alt: 1.073741824E9, Lat: 45.411322116851181, Long: -75.68433165550232, Alt: 1.073741824E9, Lat: 45.41131138801575,
RoadName: Hawthorne Ave, GeoCordinates: [Lat: 45.41175127029419, Long: -75.68276524543762, Alt: 1.073741824E9, Lat: 45.41221261024475, Long: -75.68153142929077, Alt: 1.073741824E9], NumberOfLanes: 4, Speed
RoadName: Hawthorne Ave, GeoCordinates: [Lat: 45.41237354278564, Long: -75.68110227584839, Alt: 1.073741824E9, Lat: 45.4125237464048, Long: -75.68070530891418, Alt: 1.073741824E9, Lat: 45.41264176368713
RoadName: Main St, GeoCordinates: [Lat: 45.41270613670349, Long: -75.68011522293091, Alt: 1.073741824E9, Lat: 45.41216969490051, Long: -75.67981481552124, Alt: 1.073741824E9], NumberOfLanes: 4, Speed Limit
RoadName: Smyth Rd, GeoCordinates: [Lat: 45.39899468421936, Long: -75.6645154953003, Alt: 1.073741824E9, Lat: 45.39899468421936, Long: -75.66432237625122, Alt: 1.073741824E9, Lat: 45.3989839553833, Long: -
RoadName: Smyth Rd, GeoCordinates: [Lat: 45.398930311203, Long: -75.65415143966675, Alt: 1.073741824E9, Lat: 45.39897322654724, Long: -75.65361499786377, Alt: 1.073741824E9, Lat: 45.39901614189148, Long: -
Trip ended


Trip Started
RoadName: Arthur Ln N, GeoCordinates: [Lat: 45.407127141952515, Long: -75.70547819137573, Alt: 1.073741824E9, Lat: 45.40541052818298, Long: -75.70446968078613, Alt: 1.073741824E9], NumberOfLanes: 1, Speed
RoadName: Arthur Ln N, GeoCordinates: [Lat: 45.407127141952515, Long: -75.70547819137573, Alt: 1.073741824E9, Lat: 45.40541052818298, Long: -75.70446968078613, Alt: 1.073741824E9], NumberOfLanes: 1, Speed
RoadName: Bell St N, GeoCordinates: [Lat: 45.40524959564209, Long: -75.70507049560547, Alt: 1.073741824E9, Lat: 45.40465950965881, Long: -75.70469498634338, Alt: 1.073741824E9], NumberOfLanes: 1, Speed Lim
RoadName: Arlington Ave, GeoCordinates: [Lat: 45.40558218955994, Long: -75.70387959480286, Alt: 1.073741824E9, Lat: 45.4059898853302, Long: -75.70257067680359, Alt: 1.073741824E9], NumberOfLanes: 1, Speed
RoadName: Bronson Ave, GeoCordinates: [Lat: 45.4059898853302, Long: -75.70257067680359, Alt: 1.073741824E9, Lat: 45.40573239326477, Long: -75.70242047309875, Alt: 1.073741824E9], NumberOfLanes: 4, Speed Li
RoadName: Bronson Ave, GeoCordinates: [Lat: 45.40477752685547, Long: -75.70189476013184, Alt: 1.073741824E9, Lat: 45.404638051986694, Long: -75.70180892944336, Alt: 1.073741824E9, Lat: 45.404520034790004, Lo
```

Figure 15: Example of Raw Trip Data

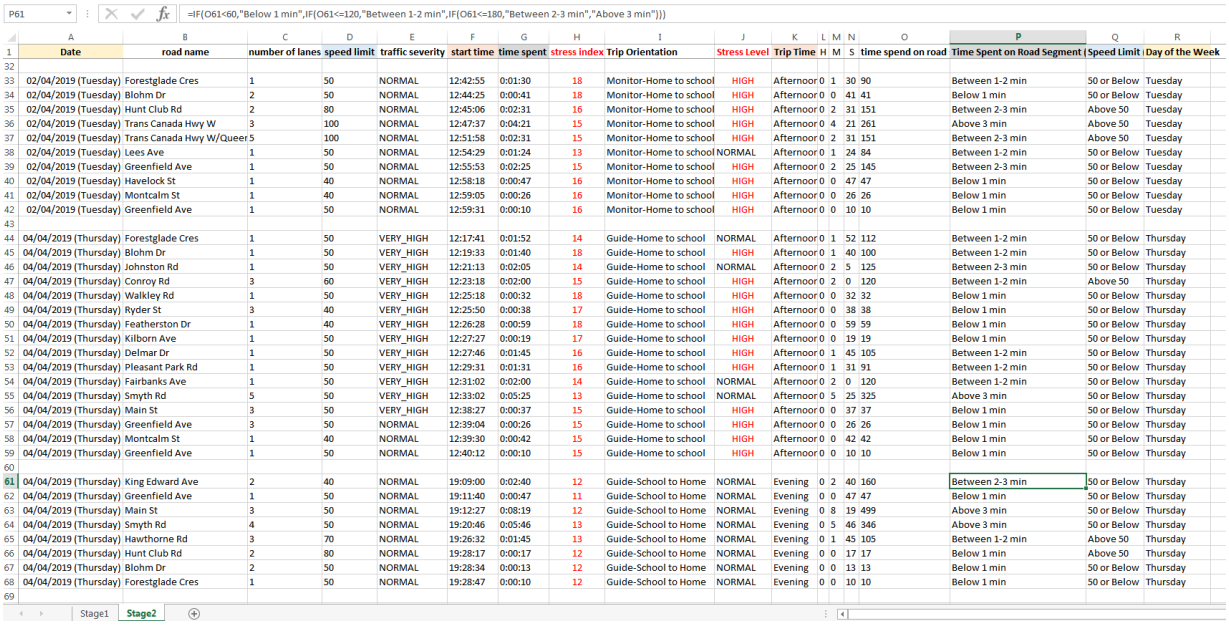

P61 =IF(O61<60,"Below 1 min",IF(O61<=120,"Between 1-2 min",IF(O61<=180,"Between 2-3 min","Above 3 min")))

	A	B	C	D	E	F	G	H	I	J	K	L	M	N	O	P	Q	R
1	Date	road name	number of lanes	speed limit	traffic severity	start time	time spent	stress index	Trip Orientation	Stress Level	Trip Time	H	M	S	time spend on road	Time Spent on Road Segment	Speed Limit	Day of the Week
32																		
33	02/04/2019 (Tuesday)	Forestglade Cres	1	50	NORMAL	12:42:55	0:01:30	18	Monitor-Home to school	HIGH	Afternoon	0	1	30	90	Between 1-2 min	50 or Below	Tuesday
34	02/04/2019 (Tuesday)	Blohm Dr	2	50	NORMAL	12:44:25	0:00:41	18	Monitor-Home to school	HIGH	Afternoon	0	0	41	41	Below 1 min	50 or Below	Tuesday
35	02/04/2019 (Tuesday)	Hunt Club Rd	2	80	NORMAL	12:45:06	0:02:31	16	Monitor-Home to school	HIGH	Afternoon	0	2	31	151	Between 2-3 min	Above 50	Tuesday
36	02/04/2019 (Tuesday)	Trans Canada Hwy W	3	100	NORMAL	12:47:37	0:04:21	15	Monitor-Home to school	HIGH	Afternoon	0	4	21	261	Above 3 min	Above 50	Tuesday
37	02/04/2019 (Tuesday)	Trans Canada Hwy W/Queer	5	100	NORMAL	12:51:58	0:02:31	15	Monitor-Home to school	HIGH	Afternoon	0	2	31	151	Between 2-3 min	Above 50	Tuesday
38	02/04/2019 (Tuesday)	Lees Ave	1	50	NORMAL	12:54:29	0:01:24	13	Monitor-Home to school	NORMAL	Afternoon	0	1	24	84	Between 1-2 min	50 or Below	Tuesday
39	02/04/2019 (Tuesday)	Greenfield Ave	1	50	NORMAL	12:55:53	0:02:25	15	Monitor-Home to school	HIGH	Afternoon	0	2	25	145	Between 2-3 min	50 or Below	Tuesday
40	02/04/2019 (Tuesday)	Havelock St	1	40	NORMAL	12:58:18	0:00:47	16	Monitor-Home to school	HIGH	Afternoon	0	0	47	47	Below 1 min	50 or Below	Tuesday
41	02/04/2019 (Tuesday)	Montcalm St	1	40	NORMAL	12:59:05	0:00:26	16	Monitor-Home to school	HIGH	Afternoon	0	0	26	26	Below 1 min	50 or Below	Tuesday
42	02/04/2019 (Tuesday)	Greenfield Ave	1	50	NORMAL	12:59:31	0:00:10	16	Monitor-Home to school	HIGH	Afternoon	0	0	10	10	Below 1 min	50 or Below	Tuesday
43																		
44	04/04/2019 (Thursday)	Forestglade Cres	1	50	VERY_HIGH	12:17:41	0:01:52	14	Guide-Home to school	NORMAL	Afternoon	0	1	52	112	Between 1-2 min	50 or Below	Thursday
45	04/04/2019 (Thursday)	Blohm Dr	1	50	VERY_HIGH	12:19:33	0:01:40	18	Guide-Home to school	HIGH	Afternoon	0	1	40	100	Between 1-2 min	50 or Below	Thursday
46	04/04/2019 (Thursday)	Johnston Rd	1	50	VERY_HIGH	12:21:13	0:02:05	14	Guide-Home to school	NORMAL	Afternoon	0	2	5	125	Between 2-3 min	50 or Below	Thursday
47	04/04/2019 (Thursday)	Conroy Rd	3	60	VERY_HIGH	12:23:18	0:02:00	15	Guide-Home to school	HIGH	Afternoon	0	2	0	120	Between 1-2 min	Above 50	Thursday
48	04/04/2019 (Thursday)	Walkley Rd	1	50	VERY_HIGH	12:25:18	0:00:32	18	Guide-Home to school	HIGH	Afternoon	0	0	32	32	Below 1 min	50 or Below	Thursday
49	04/04/2019 (Thursday)	Ryder St	3	40	VERY_HIGH	12:25:50	0:00:38	17	Guide-Home to school	HIGH	Afternoon	0	0	38	38	Below 1 min	50 or Below	Thursday
50	04/04/2019 (Thursday)	Featherston Dr	1	40	VERY_HIGH	12:26:28	0:00:59	18	Guide-Home to school	HIGH	Afternoon	0	0	59	59	Below 1 min	50 or Below	Thursday
51	04/04/2019 (Thursday)	Kilborn Ave	1	50	VERY_HIGH	12:27:27	0:00:19	17	Guide-Home to school	HIGH	Afternoon	0	0	19	19	Below 1 min	50 or Below	Thursday
52	04/04/2019 (Thursday)	Delmar Dr	1	50	VERY_HIGH	12:27:46	0:01:45	16	Guide-Home to school	HIGH	Afternoon	0	1	45	105	Between 1-2 min	50 or Below	Thursday
53	04/04/2019 (Thursday)	Pleasant Park Rd	1	50	VERY_HIGH	12:29:31	0:01:31	16	Guide-Home to school	HIGH	Afternoon	0	1	31	91	Between 1-2 min	50 or Below	Thursday
54	04/04/2019 (Thursday)	Fairbanks Ave	1	50	VERY_HIGH	12:31:02	0:02:00	14	Guide-Home to school	NORMAL	Afternoon	0	2	0	120	Between 1-2 min	50 or Below	Thursday
55	04/04/2019 (Thursday)	Smyth Rd	5	50	VERY_HIGH	12:33:02	0:05:25	13	Guide-Home to school	NORMAL	Afternoon	0	5	25	325	Above 3 min	50 or Below	Thursday
56	04/04/2019 (Thursday)	Main St	3	50	VERY_HIGH	12:38:27	0:00:37	15	Guide-Home to school	HIGH	Afternoon	0	0	37	37	Below 1 min	50 or Below	Thursday
57	04/04/2019 (Thursday)	Greenfield Ave	3	50	NORMAL	12:39:04	0:00:26	15	Guide-Home to school	HIGH	Afternoon	0	0	26	26	Below 1 min	50 or Below	Thursday
58	04/04/2019 (Thursday)	Montcalm St	1	40	NORMAL	12:39:30	0:00:42	15	Guide-Home to school	HIGH	Afternoon	0	0	42	42	Below 1 min	50 or Below	Thursday
59	04/04/2019 (Thursday)	Greenfield Ave	1	50	NORMAL	12:40:12	0:00:10	15	Guide-Home to school	HIGH	Afternoon	0	0	10	10	Below 1 min	50 or Below	Thursday
60																		
61	04/04/2019 (Thursday)	King Edward Ave	2	40	NORMAL	19:09:00	0:02:40	12	Guide-School to Home	NORMAL	Evening	0	2	40	160	Between 2-3 min	50 or Below	Thursday
62	04/04/2019 (Thursday)	Greenfield Ave	1	50	NORMAL	19:11:40	0:00:47	11	Guide-School to Home	NORMAL	Evening	0	0	47	47	Below 1 min	50 or Below	Thursday
63	04/04/2019 (Thursday)	Main St	3	50	NORMAL	19:12:27	0:08:19	12	Guide-School to Home	NORMAL	Evening	0	8	19	499	Above 3 min	50 or Below	Thursday
64	04/04/2019 (Thursday)	Smyth Rd	4	50	NORMAL	19:20:46	0:05:46	13	Guide-School to Home	NORMAL	Evening	0	5	46	346	Above 3 min	50 or Below	Thursday
65	04/04/2019 (Thursday)	Hawthorne Rd	3	70	NORMAL	19:26:32	0:01:45	13	Guide-School to Home	NORMAL	Evening	0	1	45	105	Between 1-2 min	Above 50	Thursday
66	04/04/2019 (Thursday)	Hunt Club Rd	2	80	NORMAL	19:28:17	0:00:17	12	Guide-School to Home	NORMAL	Evening	0	0	17	17	Below 1 min	Above 50	Thursday
67	04/04/2019 (Thursday)	Blohm Dr	2	50	NORMAL	19:28:34	0:00:13	12	Guide-School to Home	NORMAL	Evening	0	0	13	13	Below 1 min	50 or Below	Thursday
68	04/04/2019 (Thursday)	Forestglade Cres	1	50	NORMAL	19:28:47	0:00:10	12	Guide-School to Home	NORMAL	Evening	0	0	10	10	Below 1 min	50 or Below	Thursday
69																		

Stage1 Stage2

Figure 16: Example of Trip Stress Table

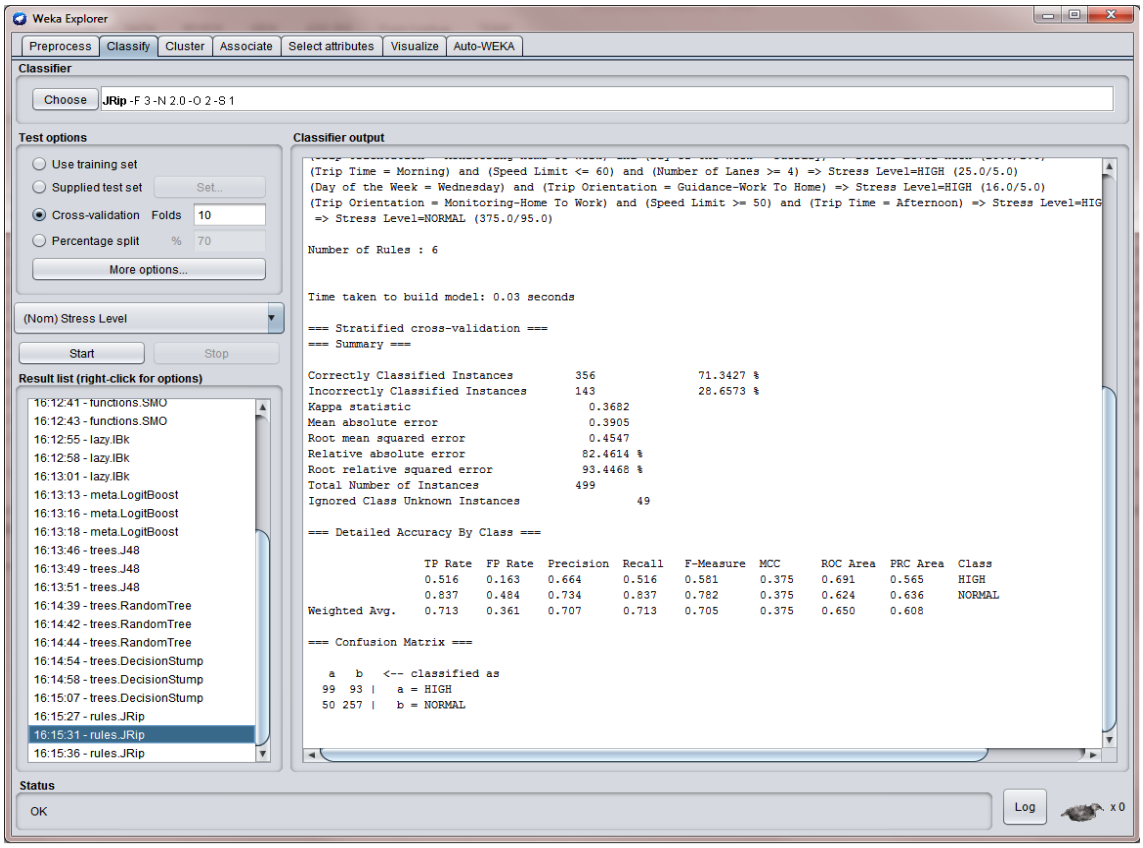

Figure 17: Example of stress prediction on Weka